Report Title:	Radically New Adsorption Cycles for Carbon Dioxide Sequestration
Report Type:	Final Report
Reporting Period Start Date:	September 1, 2003
Reporting Period End Date:	March 31, 2005
Principal Author:	James A. Ritter (PI) with Armin D. Ebner (co-PI), James A. McIntyre (PhD granted), Steven P. Reynolds (PhD candidate), and Sarang A. Gadre (PhD granted)
Report Issue Data:	October 11, 2005
DOE Award Number:	DE-FG26-03NT41799
Organization:	University of South Carolina, Department of Chemical Engineering, Columbia, SC 29208

Abstract

In Parts I and II of this project, a rigorous pressure swing adsorption (PSA) process simulator was used to study new, high temperature, PSA cycles, based on the use of a K-promoted HTlc adsorbent and 4- and 5-step (bed) vacuum swing PSA cycles, which were designed to process a typical stack gas effluent at 575 K containing (in vol%) 15 % CO_2, 75% N_2 and 10% H_2O into a light product stream depleted of CO_2 and a heavy product stream enriched in CO_2. Literally, thousands (2,850) of simulations were carried out to the periodic state to study the effects of the light product purge to feed ratio (γ), cycle step time (t_s) or cycle time (t_c), high to low pressure ratio (π_T), and heavy product recycle ratio (R_R) on the process performance, while changing the cycle configuration from 4- to 5-step (bed) designs utilizing combinations of light and heavy reflux steps, two different depressurization modes, and two sets of CO_2 -HTlc mass transfer coefficients. The process performance was judged in terms of the CO_2 purity and recovery, and the feed throughput.

The best process performance was obtained from a 5-step (bed) stripping PSA cycle with a light reflux step and a heavy reflux step (with the heavy reflux gas obtained from the low pressure purge step), with a CO_2 purity of 78.9%, a CO_2 recovery of 57.4%, and a throughput of 11.5 L STP/hr/kg. This performance improved substantially when the CO_2-HTlc adsorption and desorption mass transfer coefficients (uncertain quantities at this time) were increased by factors of five, with a CO_2 purity of 90.3%, a CO_2 recovery of 73.6%, and a throughput of 34.6 L STP/hr/kg. Overall, this preliminary study disclosed the importance of cycle configuration through the heavy and dual reflux concepts, and the importance of knowing well defined mass transfer coefficients to the performance of a high temperature PSA process for CO_2 capture and concentration from flue and stack gases using an HTlc adsorbent. This study is continuing.

Table of Contents

List of Tables

List of Figures

RR = 0.0; filled triangles – RR = 0.2; filled circles – RR = 0.4; empty squares – RR = 0.6; empty triangles – RR = 0.8. 50

Figure 13. Comparison of performance curves for the 4-step stripping PSA cycle with HR from depressurization for $\gamma = 0.5$ and θ = a) 5.8 L STP/hr/kg, b) 11.2 L STP/hr/kg and c) 17.3 L STP/hr/kg. Each line corresponds to five runs with t_s increasing from right to left. Lines: bold – $\pi_T = 4$; thin – $\pi_T = 6$; dashed – $\pi_T = 8$; dotted – $\pi_T = 10$; dot-and-dash – $\pi_T = 12$. Symbols: filled squares – RR = 0.0; filled triangles – RR = 0.2; filled circles – RR = 0.4; empty squares – RR = 0.6; empty triangles – RR = 0.8.

51

Introduction

It is now generally accepted by most climate scientists that increasing global temperatures over the last 50 years are the result of increased atmospheric concentrations of greenhouse gases such as methane (CH_4), nitrous oxide (N_2O) and, most especially, carbon dioxide (CO_2). Since the beginning of the industrial revolution, atmospheric concentrations of CO_2 have increased nearly 30%, CH_4 concentrations have more than doubled, and N_2O concentrations have risen by about 15%. These increases have enhanced the heat-trapping capability of the earth's atmosphere via the greenhouse effect. Predictions of global energy use in the next century suggest a continued increase in carbon emissions and rising concentrations of CO_2 in the atmosphere unless major changes are made in the way humans produce and use energy, in particular how humans manage carbon (Reichle et al., 1999).

There are three courses of action that can be taken to stabilize the CO_2 concentration in the atmosphere. The first approach is increased efficiency of primary energy conversion. This will decrease the amount of fossil fuels needed to provide the same energy service. The second approach is to use lower-carbon or carbon-free energy sources, with the obvious outcomes of less or no CO_2 production. The final approach is carbon sequestration, which involves the capture and storage of carbon. This last approach is probably the newest means being studied to manage CO_2 in the environment (White et al., 2003).

The most likely options for CO_2 separation and capture include (1) chemical and physical absorption, (2) physical and chemical adsorption, (3) low-temperature distillation, and (4) gas separation membranes. Among these, physical absorption using amines is currently the most widely deployed commercial technology; however, there is a significant energy penalty associated with this technology from the heat required to regenerate the solvent. Cryogenic distillation is certainly feasible and widely practiced for CO_2 recovery; but, it is only viable for CO_2 concentrations higher that 90 vol%, which is outside the range for flue gas streams. Polymeric, ceramic and metallic membranes are all viable for CO_2 recovery from flue gas streams; however, they each have their own issues involving low fluxes, degradation, fouling, cost, etc. Various adsorption processes for concentrating CO_2 from flue gas streams have also been proposed and explored, with many of the results being controversial (IEA, 1994; White et al., 2003).

An International Energy Agency (IEA, 1994) study evaluated CO_2 separation and capture using 13X zeolite in both pressure swing adsorption (PSA) and temperature swing adsorption (TSA) processes. They concluded that PSA and TSA are too energy intensive for use with gas- and coal-fired power systems. But little information was offered in the IEA study on the type of cycle employed. Nevertheless, this conclusion has led others to extrapolate these findings and further conclude that adsorption systems, in general, are not applicable for CO_2 separation and capture. It is strongly suggested that this may not be the case. It is true that the commonly studied adsorbents (e.g., zeolites and activated carbons), which have a very high capacity for CO_2 at ambient temperatures, suffer from low CO_2 capacity at elevated temperatures (Yong et al., 2002). It is also true that it may be too costly to pre-dry, cool and/or pressurize the feed and/or purge streams, which appears to be the basis for the pessimistic conclusions made in the IEA study about adsorption technology. This has not stopped research on ambient temperature

CO_2 capture by PSA, however, as evidenced by some recent studies (Gomes and Yee, 2002; Ko et al., 2003). Moreover, there are some new adsorbents, generally referred to as hydrotalcite-like compounds (HTlcs), that are selective to CO_2 at elevated temperatures, even in the presence of H_2O; and they release CO_2 simply by decreasing the pressure (Yong et al., 2002). Hence, HTlc may be a viable adsorbent for use in a high temperature PSA process for CO_2 capture.

HTlcs are anionic clays consisting of positively charged layers of metal oxides (or metal hydroxides) with inter-layers of anions, such as carbonate (Yong et al., 2002). Exchange of the metal cations, as well as intercalation of the anionic layer, allow the hydrotalcites to have stability under wet conditions and high temperatures (Ding and Alpay, 2000). Experimental results show that hydrotalcites have a reversible capacity of about 0.83 mol/kg at 575 K and 1 atm under dry or wet conditions (Yong et al., 2002). In comparison, zeolites and activated carbons have a relatively high adsorption capacity for CO_2 of 4 mol/kg and 1.5-2.5 mol/kg, respectively, at 300 K and 1 atm; however, at 575 K and 1 atm their capacities decrease substantially to about 0.10-0.25 mol/kg (Yong et al., 2002). Although, basic alumina has a CO_2 capacity ranging from 0.39 to 0.62 mol/kg under the same conditions (Yong et al., 2000), HTlcs not only exhibit a higher CO_2 capacity at elevated temperatures, but they also tend to be H_2O insensitive, which is not necessarily true for zeolites, activated carbons, and basic aluminas.

As a first step in capturing CO_2 from stack gases, the objective of Part I of this project was to study a new high temperature PSA cycle, which obviates the need to cool, dry, and pressurize the feed stream and has the potential to produce a stream enriched in CO_2 at high recovery. This new cycle was based on the use of a K-promoted HTlc adsorbent and a simple, 4-step, Skarstrom-type, vacuum swing adsorption (VSA) cycle. The four cycle steps included a cocurrent high pressure feed step, a countercurrent depressurization (vacuum) step, a countercurrent low (vacuum) pressure purge step with light product, and a countercurrent pressurization step with light product. In this case, all the cycle step times were of equal duration, which necessitated the use of four identical beds operating in succession to ensure continuous operation. Using a rigorous PSA process simulator, a parametric study was performed to examine the effects of the purge-to-feed ratio, the cycle step time (again, with all four steps of equal duration), and the pressure ratio on the process performance in terms of the CO_2 recovery (R) and CO_2 enrichment (E) at constant throughput (θ). In Part I of this report, results are reported for 125 different PSA cycle conditions.

Many PSA processes employed today use the typical 4-step, stripping cycle with light reflux described above, which is commonly referred to as the Skarstrom cycle. The word "stripping" is used here to denote that the feed is carried out at the high pressure (P_H) and the adsorbent bed strips the heavy component from the light component due to adsorption. Many modifications to this simplest of stripping PSA cycles have been developed with the number of beds varying from one to more than ten, depending on the cycle sequencing (Ruthven et al., 1994). However, a significant limitation associated with this conventional stripping PSA cycle with light reflux is that the light reflux step uses a portion of the light product gas for purge, which necessarily causes dilution of the heavy component (Liu and Ritter, 1996; Subramanian and Ritter, 1997); therefore, a pure heavy product is difficult to attain.

A number of different cycle configurations have been proposed to improve the heavy product purity or enrichment (Ruthven et al., 1994). For example, it has been shown that the addition of a cocurrent depressurization step just after the high pressure feed step improves the heavy product enrichment by allowing the heavy gas to desorb and fill the interstitial void spaces in the column while continuing to produce light product (Ruthven et al., 1994). In this way, during the subsequent countercurrent depressurization and countercurrent light reflux purge steps, the heavy product is more enriched in the heavy component. Similarly, it has been shown that the addition of a high pressure cocurrent rinse or purge step (heavy reflux step) just after the high pressure feed step improves the heavy product enrichment of this conventional PSA cycle. This heavy reflux step, as shown by two patents (Tamura, 1974; Sircar and Zondlo, 1977), recycles a portion of the heavy product gas from a low pressure column during the depressurization step, low pressure purge step, or both steps back to the high pressure column. This allows for a higher overall purity of the heavy component in the heavy product stream (Kratz et al., 1988). However, a paucity of studies have been carried out on the heavy reflux concept (Cen and Yang, 1986; Suh and Wankat, 1989; Baksh et al., 1990; Sikavitsas et al., 1995; Na et al., 2002; Olajossy et al., 2003), compared to those disclosing features of the more conventional light reflux concept (Ruthven et al., 1994). Moreover, very few of these studies have emphasized the fact that when the light reflux step is used in conjunction with the heavy reflux step in a PSA cycle configuration, in effect, a dual reflux PSA cycle has been devised.

Therefore, to further explore PSA for high temperature CO_2 capture and concentration from stack gases using a K-promoted HTlc adsorbent, the objective of Part II of this project was to study unique 4- and 5-step (bed) modifications of the simple 4-step cycle studied in Part I that take advantage of the cocurrent depressurization step and especially the heavy reflux step. In addition to the four basic PSA steps studied in part I, either a cocurrent depressurization step or a high pressure rinse (heavy reflux) step was added to the basic 4-step cycle. These additional steps were added to both 4- and 5-bed PSA process configurations by allowing for unequal cycle step durations in the former case. In this way, the effects of the new steps on the PSA process performance was discerned, with the intent of demonstrating the effectiveness of heavy and dual (light and heavy) reflux concepts for concentrating the heavy component in a feed stream. In Part II, results are reported for 2,850 different PSA cycle configurations and conditions.

Executive Summary

In Part I of this project, a rigorous pressure swing adsorption (PSA) process simulator was used to study a new, high temperature PSA cycle, based on the use of a K-promoted HTlc adsorbent and a simple, 4-step, Skarstrom-type, vacuum swing cycle. The four steps were high-pressure (P_H) adsorption with feed gas (F) just above atmospheric pressure, countercurrent depressurization (CnD) (evacuation) from P_H to a lower (vacuum) pressure (P_L), countercurrent low-pressure desorption with light product purge under vacuum (LR), and repressurization from P_L to P_H with light product gas (LPP). The heavy product (CO_2) is enriched and recovered during the CnD and LR steps, whereas the inert light product (mainly N_2 and H_2O) is recovered during the F step. The purge and pressurization gases used during the LR and LPP steps come directly from the other bed as the light product of the F, retaining their time-dependent composition and temperature.

This cycle was designed to process a typical stack gas effluent at 575 K containing (in vol%) 15 % CO_2, 75% N_2 and 10% H_2O. The effects of the purge-to-feed ratio (γ), cycle step time (t_s) (with all four steps of equal time), and pressure ratio (π_T) on the process performance was studied in terms of the CO_2 recovery (R) and CO_2 enrichment (E) at a constant throughput θ of 14.4 L STP/hr/ kg. R was defined as the number of moles of CO_2 leaving the bed during the CnD and LR steps divided by the number of moles of CO_2 entering the bed during the F step. E was defined as the average mole fraction of CO_2 leaving the bed during the CnD and LR steps divided by the mole fraction of CO_2 in the feed. Since the four cycle steps were all of equal duration in this PSA cycle, θ was defined as the amount of feed fed to one column during the F step divided by the cycle time and the mass of adsorbent in one column.

The results showed that the R increased with increasing γ and π_T and decreasing t_s, while E increased with increasing t_s and π_T and decreasing γ. The highest E of 3.9 was obtained at R = 87% and π_T = 12, whereas at R = 100% the highest E of 2.6 was obtained at π_T = 12. These results were very encouraging and show the potential of a high temperature PSA cycle for CO_2 capture. However, they also reveal the shortcomings of the 4-step, Skarstrom-type PSA cycle that only takes advantage of a light reflux step.

In Part II of this project, the rigorous pressure swing adsorption (PSA) process simulator was used further to study six different high temperature PSA cycles for concentrating CO_2 from the same stack gas effluent using K-promoted HTlc. These cycles included a 4-step cycle with a LR, a 5-step cycle with LR and cocurrent depressurization (CoD) and CnD, a 4-step cycle with LR and CoD and CnD, a 5-step cycle with LR and heavy reflux (HR) from depressurization, a 5-step cycle with LR and HR from purge, and a 4-step cycle with HR from depressurization. Not only were the effects of γ, t_s, and π_T on the process performance studied in terms of the CO_2 recovery (R), CO_2 purity ($y_{CO2,avg}$) in the heavy product stream, and feed throughput (θ), but also the effects of different cycle configurations under similar conditions and the effects of the adsorption and desorption mass transfer coefficients (k_a and k_d) for the same cycle configuration and conditions were also examined.

The results from Part II of this study showed that a dual reflux (LR and HR) PSA process configuration provided the best performance. A careful examination of the results provided clear

evidence about the use of a HR step, but only when combined with a LR step, with any cycle having a HR step far outperforming any cycle with only a LR step. In terms of CO_2 purity, the dual reflux, 5-step stripping PSA cycle with LR and HR from purge performed the best, especially when the mass transfer coefficients were increased by a factor of five. The former process resulted in a CO_2 purity of 78.9%, a CO_2 recovery of 57.4%, and a throughput of 11.5 L STP/hr/kg, which improved substantially a CO_2 purity of 90.3%, a CO_2 recovery of 73.6%, and a throughput of 34.6 L STP/hr/kg simply by increasing the CO_2-HTlc adsorption and desorption mass transfer coefficients (uncertain quantities at this time) by factors of five. The next best PSA cycle was the dual reflux, 5-step stripping PSA cycle with LR and HR from depressurization. In general, the single reflux, 4-step or 5-step stripping PSA cycles with LR or HR did not perform that well in terms of producing a heavy product steam enriched in CO_2. This was the case even when a cocurrent depressurization step was included with the LR cycle or even when the mass transfer coefficients were increased by factors of five for the 4-step stripping PSA cycle with LR. The question that will be addressed over the next three years is how to improve the performance of this dual reflux process in terms of increasing the CO_2 purity, CO_2 recovery and feed throughput through creative PSA cycle design configuration. With the results of this study also suggesting that mass transfer plays a key role in improving the PSA process performance, as demonstrated by increasing the mass transfer coefficients by factors of five, another question that will be addressed over the next three years is how to accurately measure the mass transfer properties of the K-promoted HTlc adsorbent.

Process Description

In Part I, the PSA cycle consisted of four interconnected beds each undergoing four cycle steps of equal duration in succession. Note that if the four step times were not of equal duration, but chosen in such a way that some steps were shorter than other steps, then a PSA cycle with less than four beds could have been devised. However, this cycle configuration would necessarily have a different process performance than that of a similar PSA cycle with equal step times. Equal step times were chosen here to make this particular parametric study more understandable in terms of the factors that control the process performance. In Part II of this report, some cycle configurations with unequal step times are investigated.

The four steps were high-pressure (P_H) adsorption with feed gas (F) just above atmospheric pressure, countercurrent depressurization (evacuation) from P_H to a lower (vacuum) pressure (P_L) (CnD), countercurrent low-pressure desorption with light product purge under vacuum (LR), and repressurization from P_L to P_H with light product gas (LPP). The heavy product (CO_2) is enriched and recovered during the CnD and LR steps, whereas the inert light product (mainly N_2 and H_2O) is recovered during the F step. The purge and pressurization gases used during the LR and LPP steps come directly from one of the other beds as the light product produced during the F step, while retaining their time-dependent composition and temperature. This 4-step light reflux, stripping PSA cycle is shown schematically in Figure 1a.

The periodic state PSA process performance of this cycle was judged by the CO_2 recovery (R), CO_2 enrichment (E), and feed throughput (θ). R was defined as the number of moles of CO_2 leaving the bed during the CnD and LR steps divided by the number of moles of CO_2 entering the bed during the F step. E was defined as the average mole fraction of CO_2 leaving the bed during the CnD and LR steps divided by the mole fraction of CO_2 in the feed. Since the four cycle steps were all of equal duration in this PSA cycle, θ was defined as the amount of feed fed to one column during the F step divided by the cycle time and the mass of adsorbent in one column.

In Part II, five additional PSA cycles were studied. In addition to the classic 4-step, light reflux (LR), stripping cycle depicted in Figure 1a, they ranged from a 4- and 5-step variations of this cycle with cocurrent depressurization (Figure 1b and 1c) to 5-step LR and heavy reflux (HR), i.e., dual reflux, stripping cycles (Figure 1d and 1e) to a 4-step HR stripping cycle (1f). The 5-step stripping PSA cycle depicted in Figure 1b, with both cocurrent and countercurrent depressurization steps, includes the following cycle steps: high-pressure (P_H) adsorption with feed gas (F) just above atmospheric pressure, cocurrent depressurization (evacuation) from P_H to some intermediate pressure P_I (CoD), countercurrent depressurization (evacuation) from P_I to a lower (vacuum) pressure (P_L) (CnD), countercurrent low-pressure desorption with light product purge under vacuum (LR), and repressurization from P_L to P_H (LPP) with light product gas. The heavy product (CO_2) is enriched and recovered during the CnD and LR steps, whereas the inert light product (mainly N_2 and H_2O) is recovered during the F and CoD steps. The purge and pressurization gases used during the LR and LPP steps come directly from one of the other beds as the light product of the F step, while retaining their time-dependent composition and temperature. The 4-step PSA cycle depicted in Figure 1c, again with both cocurrent and countercurrent depressurization steps, is similar to the 5-step cycle just described, except that it is

able to operate with one less bed by carrying out the CoD and CnD steps in succession, but with each having half the duration of the other three cycle steps.

The 5-step stripping PSA cycle depicted in Figure 1d, with both light and heavy reflux steps (a dual reflux PSA cycle), includes the following cycle steps: high-pressure (P_H) adsorption with feed gas (F) just above atmospheric pressure, high pressure rinse with heavy reflux (HR) obtained from one of the other columns undergoing depressurization, countercurrent depressurization (evacuation) from P_H to a lower (vacuum) pressure (P_L) (CnD), countercurrent low-pressure desorption with light product purge under vacuum (LR), and repressurization from P_L to P_H (LPP) with light product gas. The heavy product (CO_2) is enriched and recovered during the CnD and LR steps, whereas the inert light product (mainly N_2 and H_2O) is recovered during the F and HR steps. The purge and pressurization gases used during the LR and LPP steps come directly from one of the other beds as the light product of the F step, retaining their time-dependent composition and temperature. The 5-bed PSA cycle depicted in Figure 1e, again with both light and heavy reflux steps (a dual reflux PSA cycle), is similar to the 5-bed cycle just described, except that the HR gas comes from the light product gas instead of the depressurization gas as shown. The 4-step PSA cycle depicted in Figure 1f, with only a heavy reflux step, is similar to the 5-step cycles just described, except that it is able to operate with one less bed by not carrying out the LR step, which necessarily forces the HR gas to be obtained from the depressurization step as shown.

The periodic state PSA process performances of these cycles are again judged by the CO_2 recovery (R), CO_2 purity in vol% or equivalently mol%, and feed throughput (θ). R was defined as the number of moles of CO_2 leaving the bed during the steps where heavy product (HP) was withdrawn from the system divided by the number of moles CO_2 entering the bed in the feed. The CO_2 purity was defined as the average mole fraction of CO_2 leaving the bed during the steps where heavy product (HP) was withdrawn from the system. θ was defined here as the total amount of feed fed to the process during one complete cycle divided by the total cycle time and the mass of adsorbent in all the columns because not all the cycle steps were of equal duration.

Mathematical Model

The multicomponent PSA model used for this project was similar to that previously developed by Ritter and co-workers (Liu et al., 1999; Liu et al., 2000). The following assumptions were made in this model: the ideal gas law applies, the heat of adsorption is independent of temperature and adsorbed phase loading, the heat capacity of the solid is constant, the heat transfer with the surroundings is described by an average heat transfer coefficient that is constant, the compression and expansion of the gas between the high and low pressures are done isothermally, the pressure drop within the columns is considered negligible, and the linear driving force (LDF) mass transfer model is considered applicable. The total porosity of the bed is also considered and modified by the following equation.

$$\varphi = \sum_{i=1}^{N} \frac{q_i \rho_p MW_i}{\rho_{a,i}} \tag{1}$$

As the loading increases in the pores of the adsorbent, the adsorbed phase occupies a small, but increasing, portion of the volume of the pore. Therefore, φ can be thought of as a capacitance inside of the pore that depends on the loading of component i (q_i), the particle density (ρ_p), the molecular weight of component i (MW_i), and the adsorbed density of component i ($\rho_{a,i}$). The adsorbed phase density is assumed to have the same density as the liquid phase of the particular component.

For an *N* component process, the component mass balances are given by

$$\frac{\varepsilon + (1-\varepsilon)(\chi - \varphi)}{\varepsilon} \frac{\partial y_i}{\partial t} + u \frac{\partial y_i}{\partial z} - y_i \sum_{j=1}^{N} S_j + S_i = 0 \qquad i = 1, 2, \ldots, N\text{-}1 \tag{2}$$

where

$$S_i = \frac{1-\varepsilon}{\varepsilon} \frac{RT\rho_p}{P} \frac{\partial q_i}{\partial t} \qquad i = 1, 2, \ldots, N \tag{3}$$

and with the constraint that

$$\sum_{i=1}^{N} y_i = 1 \tag{4}$$

The $\frac{\partial q_i}{\partial t}$ term is based on the LDF approximation as

$$\frac{\partial q_i}{\partial t} = k_i \left(q_i^* - q_i \right) \qquad i = 1, 2, \ldots, N \tag{5}$$

The total mass balance becomes

$$\frac{\partial u}{\partial z} - \frac{u}{T}\frac{\partial T}{\partial z} + \frac{\varepsilon + (1-\varepsilon)(\chi - \varphi)}{\varepsilon} \left(\frac{1}{P}\frac{\partial P}{\partial t} - \frac{1}{T}\frac{\partial T}{\partial t} \right) - \frac{(1-\varepsilon)}{\varepsilon}\frac{\partial \varphi}{\partial t} + \sum_{i=1}^{N} S_i = 0 \tag{6}$$

where

$$\frac{\partial \varphi}{\partial t} = \sum_{i=1}^{N} \frac{\frac{\partial q_i}{\partial t} \rho_p MW_i}{\rho_{a,i}} \tag{7}$$

The energy balance is given by

$$\frac{\varepsilon+(1-\varepsilon)(\chi-\varphi)}{\varepsilon}C_{P,g}\frac{\partial T}{\partial t}+uC_{P,g}\frac{\partial T}{\partial z}+\frac{2h}{\varepsilon r_b}\frac{RT}{P}(T-T_0)+$$
$$\frac{1-\varepsilon}{\varepsilon}\frac{RT}{P}\rho_P\sum_{i=1}^{N}\left(C_{P,a,i}q_i\frac{\partial T}{\partial t}+\Delta H_i\frac{\partial q_i}{\partial t}\right)+\rho_p C_{P,p}\frac{1-\varepsilon}{\varepsilon}\frac{RT}{P}\frac{\partial T}{\partial t}=0 \quad (8)$$

The heat capacity of the gas, $C_{P,g}$, has a dependence on temperature and the mole fraction of the components as shown by

$$C_{P,g}=\sum_{i=1}^{N}y_i C_{P,g,i} \quad (9)$$

where

$$C_{P,g,i}=A_i+B_iT+C_iT^2+D_iT^3 \quad (10)$$

The adsorbed phase heat capacity of each component is assumed to be equal to the gas phase heat component, so $C_{P,a,i}$ is equal to $C_{P,g,i}$.

The equilibrium amount adsorbed for each component in the gas phase is predicted by a Langmuir isotherm.

$$q_i^*=\frac{q_i^s b_i P y_i}{1+\sum_{i=1}^{N}b_i P y_i} \quad (11)$$

where

$$q_i^s=q_{i,1}^s T+q_{i,2}^s \quad (12)$$

and

$$b_i=b_i^0\exp\left(\frac{B_i^0}{T}\right) \quad (13)$$

However, in this model only the adsorption of CO_2 is considered, as the adsorption of N_2 and H_2O are considered to be inert for the K-promoted HTlc adsorbent.

The pressure history during a cycle is assumed to be a known function of time; hence, it is input to the model. During the feed, heavy reflux, and light reflux steps, the pressure is constant and set at P_H, P_H and P_L, respectively. During the depressurization and pressurization steps, however, the pressure changes with time, but with the constraint that the desired intermediate pressure for cocurrent depressurization (P_I), the low pressure for countercurrent depressurization (P_L), and the high pressure for pressurization (P_H) are always reached by the end of a pressure changing step.

The function that describes how the pressure changes with time during the pressurization step is a non-linear function of time *t* and has the following form:

$$P=\frac{2\left(P^*-P_L\right)}{1+\exp\left(-ct\right)}-P^*+2P_L \quad (14)$$

where

$$P^* = \frac{P_H + 2P_L\left(\frac{1}{1+\exp(-ct_s)}\right) - 1}{\frac{2}{1+\exp(-ct_s)} - 1} \tag{15}$$

and

$$c = \frac{2r_P}{P_H - P_L} \tag{16}$$

P_H is the high pressure, P_L is the low pressure, t_s is the cycle step time, and r_P is the initial pressurization rate. This very well behaved function was used to provide a more realistic, non-linear pressurization rate, especially during the long cycle time simulations. For use, it simply requires a specification of r_P, which was chosen to be 5.0 kPa/s for all simulations. The function that describes how the pressure changes with time during the depressurization steps is a linear function of time and has the following form:

$$P = P_i - \frac{(P_i - P_f)}{t_s}t \tag{17}$$

where P is the pressure at any time t, P_i is the initial pressure of the step, P_f is the final pressure of the step, t_s is the time for the pressure changing step, and t is the time into this step. The initial pressure is always P_H for the cocurrent depressurization step. However, the initial pressure is one of two values for the countercurrent depressurization step. For the cycles that incorporate a cocurrent depressurization step, the initial pressure of the countercurrent depressurization step is some specified intermediate pressure P_I. For the cycle that does not have a cocurrent depressurization step, the initial pressure of the countercurrent depressurization step is P_H. The final pressure of the cocurrent depressurization step is always some specified intermediate pressure P_I, while the final pressure for the countercurrent depressurization step is always the low pressure P_L.

The initial and boundary conditions depend on the PSA cycle configuration being studied. All simulations start from clean beds; therefore, the initial conditions for all of the different PSA cycles are:

F:	at t = 0:	$y_i = 0$,	$y_{N2} = 1$,	$T=T_o$,	$q_i=0$,	for all z

For subsequent cycles, the initial and boundary conditions for each step in the 4-step stripping PSA cycle with light reflux are:

F:	at t = 0:	$y_i = y_{i,LPP}$,	$T = T_{LPP}$,	$q_i=q_{i,LPP}$,	for all z
	at z = 0:	$y_i = y_{i,f}$,	$T = T_f$,	$u = u_f$,	for all t
CnD:	at t = 0:	$y_i = y_{i,F}$,	$T = T_F$,	$q_i=q_{i,F}$,	for all z
	at z = L:	$u = 0$,			for all t
LR:	at t = 0:	$y_i = y_{i,CnD}$,	$T = T_{CnD}$,	$q_i=q_{i,CnD}$,	for all z
	at z = L:	$y_i = y_{i,F}(t)$,	$T = T_F(t)$,	$u = u_{LR}$,	for all t
LPP:	at t = 0:	$y_i = y_{i,LR}$,	$T = T_{LR}$,	$q_i=q_{i,LR}$,	for all z
	at z = 0:	$u = 0$,			for all t

When the cocurrent depressurization step is used with the 4- or 5-step stripping PSA cycles with light reflux, the following initial and boundary conditions apply.

F:	at t = 0:	$y_i = y_{i,LPP}$,	$T = T_{LPP}$,	$q_i = q_{i,LPP}$,	for all z
	at z = 0:	$y_i = y_{i,f}$,	$T = T_f$,	$u = u_f$,	for all t
CoD:	at t = 0:	$y_i = y_{i,F}$,	$T = T_F$,	$q_i = q_{i,F}$,	for all z
	at z = 0:	$u = 0$,			for all t
CnD:	at t = 0:	$y_i = y_{i,CoD}$,	$T = T_{CoD}$,	$q_i = q_{i,CoD}$,	for all z
	at z = L:	$u = 0$,			for all t
LR:	at t = 0:	$y_i = y_{i,CnD}$,	$T = T_{CnD}$,	$q_i = q_{i,CnD}$,	for all z
	at z = L:	$y_i = y_{i,F}(t)$,	$T = T_F(t)$,	$u = u_{LR}$,	for all t
LPP:	at t = 0:	$y_i = y_{i,LR}$,	$T = T_{LR}$,	$q_i = q_{i,LR}$,	for all z
	at z = 0:	$u = 0$,			for all t

The 5-step stripping PSA cycle with light reflux and heavy reflux (from depressurization) has the following initial and boundary conditions:

F:	at t = 0:	$y_i = y_{i,LPP}$,	$T = T_{LPP}$,	$q_i = q_{i,LPP}$,	for all z
	at z = 0:	$y_i = y_{i,f}$,	$T = T_f$,	$u = u_f$,	for all t
HR:	at t = 0:	$y_i = y_{i,F}$,	$T = T_F$,	$q_i = q_{i,F}$,	for all z
	at z = 0:	$y_i = y_{i,CnD}(t)$,	$T = T_{CnD}(t)$,	$u = u_{HR}$,	for all t
CnD:	at t = 0:	$y_i = y_{i,HR}$,	$T = T_{HR}$,	$q_i = q_{i,HR}$,	for all z
	at z = L:	$u = 0$,			for all t
LR:	at t = 0:	$y_i = y_{i,CnD}$,	$T = T_{CnD}$,	$q_i = q_{i,CnD}$,	for all z
	at z = L:	$y_i = y_{i,F}(t)$,	$T = T_F(t)$,	$u = u_{LR}$,	for all t
LPP:	at t = 0:	$y_i = y_{i,LR}$,	$T = T_{LR}$,	$q_i = q_{i,LR}$,	for all z
	at z = 0:	$u = 0$,			for all t

The initial and boundary conditions for the 5-step stripping PSA cycle with light reflux and heavy reflux (from purge) are:

F:	at t = 0:	$y_i = y_{i,LPP}$,	$T = T_{LPP}$,	$q_i = q_{i,LPP}$,	for all z
	at z = 0:	$y_i = y_{i,f}$,	$T = T_f$,	$u = u_f$,	for all t
HR:	at t = 0:	$y_i = y_{i,F}$,	$T = T_F$,	$q_i = q_{i,F}$,	for all z
	at z = 0:	$y_i = y_{i,LR}(t)$,	$T = T_{LR}(t)$,	$u = u_{HR}$,	for all t
CnD:	at t = 0:	$y_i = y_{i,HR}$,	$T = T_{HR}$,	$q_i = q_{i,HR}$,	for all z
	at z = L:	$u = 0$,			for all t
LR:	at t = 0:	$y_i = y_{i,CnD}$,	$T = T_{CnD}$,	$q_i = q_{i,CnD}$,	for all z
	at z = L:	$y_i = y_{i,F}(t)$,	$T = T_F(t)$,	$u = u_{LR}$,	for all t
LPP:	at t = 0:	$y_i = y_{i,LR}$,	$T = T_{LR}$,	$q_i = q_{i,LR}$,	for all z
	at z = 0:	$u = 0$,			for all t

Finally, the 4-step stripping PSA cycle with light reflux and heavy reflux (from depressurization) has the following initial and boundary conditions:

F:	at t = 0:	$y_i = y_{i,LPP}$,	$T = T_{LPP}$,	$q_i = q_{i,LPP}$,	for all z
	at z = 0:	$y_i = y_{i,f}$,	$T = T_f$,	$u = u_f$,	for all t
HR:	at t = 0:	$y_i = y_{i,F}$,	$T = T_F$,	$q_i = q_{i,F}$,	for all z
	at z = 0:	$y_i = y_{i,CnD}(t)$,	$T = T_{CnD}(t)$,	$u = u_{HR}$,	for all t
CnD:	at t = 0:	$y_i = y_{i,HR}$,	$T = T_{HR}$,	$q_i = q_{i,HR}$,	for all z
	at z = L:	$u = 0$,			for all t
LPP:	at t = 0:	$y_i = y_{i,CnD}$,	$T = T_{CnD}$,	$q_i = q_{i,CnD}$,	for all z

at z = 0: u = 0, for all t

Using the in-house developed PSA process simulator code, each simulation was carried out to the periodic state, which is defined as that state wherein none of the dependent variables change within a set tolerance from cycle to cycle. Periodic behavior was typically achieved for each set of PSA process conditions and cycle configuration after carrying out 200 to 300 cycles.

Physical Properties

The bed characteristics, gas phase species and HTlc adsorbent transport and thermodynamic properties used in the mathematical model are shown in Table 1. Figure 2 shows the experimental adsorption isotherm data for CO_2 on a K-promoted HTlc at four different temperatures (Ding and Alpay, 2000, 2001). These data were fitted to the temperature dependent Langmuir isotherm model shown in the figure and depicted by Equations 10 to 12. The isosteric heat of adsorption, ΔH_i, was estimated from the temperature dependence of the isotherm parameter, b_i.

The adsorption and desorption mass transfer coefficients for CO_2 with this HTlc adsorbent were taken from the work of Ding and Alpay (2001). The other components in the system were considered to be inert for this adsorbent; therefore, the mass transfer coefficients for N_2 and H_2O were set to zero. The bench-scale column radius (r_b) and length (L), and corresponding heat transfer coefficient, h, were taken from an experimental setup described by Liu et al. (1998).

Results and Discussion

Part I: Parametric Study with a 4-Step Stripping PSA Cycle with Light Reflux

A total of 125 simulations were carried out, all at constant throughput θ = 14.4 L STP/hr kg, using the process configuration shown in Figure 1a for the 4-bed stripping PSA cycle with light reflux. Table 2 provides the fixed and varied process parameters studied in Part I. At each of the five pressure ratios, five cycle step times and five purge to feed ratios were investigated. The base case conditions for the purge to feed ratio (γ), cycle step time (t_s), and pressure ratio ($\pi_T = P_H/P_L$) are underlined in Table 2. With the feed flow rate (V_f) fixed at 1.0 L STP/min, γ was changed by changing the purge flow rate; and with P_H fixed at 137.9 kPa, π_T was changed by changing P_L. All simulations were started from a clean bed containing only inert gas and carried out until the periodic state was reached. The results from 15 simulations carried out at the base case conditions (i.e., γ = 0.75, t_s = 300 s and π_T = 8 for the base case, non-varying parameters) are shown in Figure 3. Qualitatively similar trends were observed for conditions outside of the base case conditions (not shown).

Figure 3a shows the effect of γ on R and E with π_T = 8 and t_s = 300 s. R increased, but E decreased, as γ increased. Since the purge gas was taken from the light product gas and used to sweep the low pressure column during the countercurrent purge step, more CO_2 left the column as enriched product. Also, the light product purge regenerated the adsorbent; thus, the adsorbent was able to adsorb more CO_2 in the subsequent adsorption step, thereby allowing less CO_2 to breakthrough into the light product. Both caused R to increase with increasing γ. However, since more of the light product was returned to the low pressure column as purge with increasing γ, it diluted the CO_2 in the heavy product, which caused E to decrease with increasing γ.

Figure 3b shows the effect of t_s on R and E with π_T = 8 and γ = 0.75. R decreased, but E increased, as t_s increased. Since CO_2 entered the column during the feed step, more CO_2 entered the system as t_s increased; thus, it was more likely for CO_2 to breakthrough into the light product, which decreased R with increasing t_s. However, as more CO_2 entered the system, more CO_2 was adsorbed by the hydrotalcite; hence, more CO_2 desorbed during the depressurization and low pressure purge steps and exited the system in the enriched product gas, which caused E to increase with increasing t_s.

Figure 3c shows the effect of π_T on R and E with t_s = 300 s and γ = 0.75. Both R and E increased with increasing π_T. Since t_s and P_H were fixed, the amount of CO_2 entering the system during the feed step was also fixed. Hence, the observed increases in R and E with increasing π_T were actually caused by P_L decreasing, i.e., a deeper vacuum was being applied to the system, which had two effects. For a fixed γ (i.e., the ratio of the purge gas to feed gas velocities), a lower P_L meant less purge gas was used to clean the bed, which caused R to increase. The use of less purge gas also resulted in less dilution of the heavy product, which caused E to increase. In effect, the working capacity of the adsorbent increased, because larger pressure swings allowed for a greater change in the loading, as gleaned from the large slope changes in the low pressure regions of the HTlc isotherms shown in Figure 1.

The results in Figure 3, not surprisingly, implied that a compromise exists between the

CO_2 recovery and enrichment. In other words, the set of PSA process conditions that simultaneously maximizes both R and E is not necessarily the same set of conditions that maximizes R or E independently. The results in Figure 4, which show the effect of the purge to feed ratio (γ) and cycle step time (t_s) on the (a) CO_2 recovery (R) and (b) CO_2 enrichment (E) for 25 simulations carried out at a pressure ratio π_T = 8 and throughput θ = 14.4 L STP/hr/kg, in terms of 3-D contour plots tend to reveal the conditions that produce this optimum behavior better than simple 2-D plots (Figure 3). The results in Figure 4a clearly show that R increased monotonically with increasing γ and decreasing t_s with R = 100% for numerous sets of conditions. In contrast, the results in Figure 4b reveal much more complex behavior: E increased monotonically with increasing γ, but only at the lower values of t_s; it clearly went through a maximum at the higher values of t_s. Moreover, at the lower values of γ, E decreased with decreasing t_s, whereas at the higher values of γ, E increased with increasing t_s. Nevertheless, it is clear that a set of γ and t_s exists that maximizes both R and E, an effect that could not be ascertained from Figure 3.

The results in Figure 4 provide a convenient, but somewhat limited methodology, to evaluate the simulations, because only a fraction of them can be plotted. The results from all 125 simulations are easily evaluated, however, by constructing a plot or R versus E, as shown in Figure 5. Performance curves are shown for a feed flow rate of 1.0 L STP/min (i.e., θ = 14.4 L STP/hr/kg). Each line corresponds to five runs with t_s increasing from right to left. Each family of lines correspond to a constant γ with π_T increasing as their fan spreads from left to right. From this graph, it is easy to pinpoint the conditions that maximize both R and E. In this case, an E = 3.89 at R = 86.8% was obtained with γ = 0.5, t_s = 500 s and π_T = 12, which correspond to the smallest γ, longest t_s and highest π_T investigated, possibly an expected outcome with a bit of hindsight. The conditions that optimized E or R independently clearly were not the same, but could readily be identified from such a plot. For example, the best CO_2 enrichment dropped to E = 2.79 to achieve an R = 99.99%, but now with γ = 1.5, t_s = 400 s and π_T = 12. Since all 125 simulations were obtained at the same throughput θ, other θs would shift these lines accordingly.

In summary, a rigorous PSA process simulator was used in Part I to study a new, high temperature PSA cycle, based on the use of a K-promoted HTlc adsorbent and a simple, 4-step, Skarstrom-type, vacuum swing adsorption cycle designed to process a typical stack gas effluent at 575 K containing (in vol%) 15 % CO_2, 75% N_2 and 10% H_2O. The effects of the purge-to-feed ratio (γ), cycle step time (t_s) (with all four steps of equal time), and pressure ratio (π_T) on the process performance was studied in terms of the CO_2 recovery (R) and enrichment (E) at a constant throughput θ of 14.4 L STP/hr/ kg. The results from 125 simulations, carried out at five different purge-to-feed ratios, cycle step times and pressure ratios showed that R increased with increasing γ and π_T and decreasing t_s, while E increased with increasing t_s and π_T and decreasing γ. The highest E of 3.9 was obtained at R = 87% with γ = 0.5, π_T = 12 and t_s = 500 s, apparent optimum conditions for both R and E. In contrast, at R = 100% the highest E of 2.8 was obtained at γ = 1.5, π_T = 12 and t_s = 500 s, apparent optimum conditions for R but not E. Different feed flow rates, i.e., different θs, would result in different sets of optimum, possibly better conditions. Hence, these results were very encouraging and showed the potential of a high temperature PSA cycle for CO_2 capture. Part II of this study provides a comprehensive analysis of six different stripping PSA cycles that take advantage of different modes of reflux, i.e., light,

heavy and dual (light and heavy) reflux steps, to concentrate the heavy component in a feed stream, in this case the CO_2.

Part II: Study of Six Stripping PSA Cycles with Various Reflux Steps

Literally, thousands of simulations of six different PSA process configurations and two sets of mass transfer coefficients (those listed in Table 1 and five times those values, denoted as k = 5k in subsequent tables) were carried out using the in-house developed stripping PSA process simulator. Again, the six different PSA cycle configurations are shown in Figure 1. Table 3 indicates the ranges of process conditions studied for each of the six PSA cycle configurations. Table 4 indicates the range of performances achieved in terms of feed throughput, and CO_2 purity and recovery for a given PSA cycle configuration and the range of process conditions studied. Table 5 provides a summary of the best performances, based on the highest CO_2 purity obtained for a given PSA cycle configuration and set of corresponding conditions. Note the rows for the cases where the adsorption and desorption mass transfer coefficients were each increased by a factor of five, denoted by k = 5k in Tables 3 to 5.

4-Step Stripping PSA Cycle with Light Reflux: Throughputs ranging from 3.6 to 43.2 L STP/kg/hr were studied with this PSA cycle, as indicated in Tables 3 to 5. Figures 6a to 6f show the effect of the throughput, varying from 10.8 to 28.8 L STP/kg/hr, on the process performance of the 4-Bed stripping PSA cycle with light reflux (Figure 1a). Within each figure, five pressure ratios, five cycle step times and five purge to feed ratios were also investigated. The values of these parameters are the same as those studied in Part I and provided in Table 2, with the range provided in Table 3. The effects of these parameters can be observed from a careful examination of each figure within Figure 6; however, since the interpretation is the same as presented in Part I of this study, it is not discussed any further in this section. Tables 3, 4 and 5 respectively show the ranges of the process conditions, the corresponding ranges of the resulting performances, and the conditions that resulted in the best performance of this 4-bed stripping PSA cycle with light reflux.

It was relatively easy to find conditions were 100% recovery of CO_2 was achieved over a broad range of throughputs up to 14.4 L STP/hr/kg (Figures 6a and 6b). This was due to the column being long enough to avoid breakthrough of CO_2 into the light product stream under these conditions. However, for the higher throughputs, breakthrough of CO_2 into the light product stream was eminent and the recoveries systematically decreased as the throughput increased, as noticed by comparing the results in Figures 6c to 6f. The results in Table 4 show very clearly that the maximum CO_2 purity was limited to 49.4 % at a CO_2 recovery of 100% for this typical 4-bed stripping PSA cycle with light reflux (θ = 7.2 L STP/hr/kg, γ = 0.75, t_s = 500 s and π = 12). However, these are not the conditions that maximize the purity. The results in Tables 4 and 5 also show very clearly that to increase the CO_2 purity to the maximum value obtainable with this cycle under these conditions, which was 66.4 %, the CO_2 recovery was limited to 69.8% (θ = 21.6 L STP/hr/kg, γ = 0.50, t_s = 500 s and π = 12). Notice that to achieve higher purities, the bed must be either loaded up with more CO_2 during adsorption or depleted of more CO_2 during desorption. The former necessarily requires higher feed flow rates or longer cycle times, with both causing the CO_2 recovery to decrease. The later necessarily requires higher pressure ratios (lower P_L with P_H fixed) or lower purge to feed ratios, with the former and

later causing the CO_2 recovery to increase and decrease, respectively. Again, these effects can all be gleaned from the trends observed in Figure 6.

Evidence in the literature (Soares et al., 2004) suggests that the mass transfer coefficients (k_a and k_d) of CO_2 on K-promoted HTlc may be significantly larger than those shown in Table 1. Since there is a dispute as to the magnitude of the adsorption and desorption mass transfer coefficients, simulations were also run with the k_a and k_d increased to five times the values listed in Table 1. The results are displayed in Figure 7 for $\gamma = 0.5$ and for a range of throughputs from 7.2 to 43.2 L STP/kg/hr. The higher mass transfer coefficients increase both the CO_2 recovery and the CO_2 purity; but, the effect was most pronounced on the recovery, especially at the higher throughputs. With the higher mass transfer coefficients, more of the heavy component was adsorbed and desorbed during the cycle. Thus, during adsorption less CO_2 was lost in the light product improving R. Since more CO_2 was adsorbed during the feed step, more CO_2 was desorbed during the CnD and LR steps and exited the bed in the enriched product gas, which caused the heavy product purity to also increase. As an example, from Figure 7b, R improved from 84.0% to 98.7% while the purity increased from 64.0% to 66.8% for $\theta = 14.4$ L STP/hr/kg, $\pi_T = 12$, $\gamma = 0.5$ and $t_s = 500$ s. The results in Table 4 show very clearly that the maximum CO_2 purity was still limited to 64.2 % at a CO_2 recovery of 100% for this typical 4-bed stripping PSA cycle with light reflux. However, these are not the conditions that maximize the purity. The results in Tables 4 and 5 also show very clearly that to increase the CO_2 purity to the maximum value obtainable with this cycle under these increased mass transfer conditions, which was 73.5 %, the CO_2 recovery was limited to 89.2 % ($\theta = 43.2$ L STP/hr/kg, $\pi_T = 12$, $\gamma = 0.5$ and $t_s = 500$ s, Figure 7e). This performance was much better than that achieved with the diminished mass transfer coefficients, with all three performance indicators markedly improving (Table 5). Clearly, accurate mass transfer coefficients are needed to ensure that the PSA simulations provide realistic information.

Based on these results and the previous results for this 4-step stripping PSA cycle with light reflux, it is becoming apparent that it is not possible to achieve a CO_2 purity of 100% with this cycle, irrespective of the recovery. Hence, this cycle must be modified in some way to improve the purity without diminishing the throughput and recovery. Five modifications of this cycle were studied in an attempt to achieve this goal. The results are provided below.

4-Step and 5-Step Stripping PSA Cycles with LR and CoD and CnD: One way to increase the purity obtained from the 4-bed stripping PSA cycle with light reflux (LR) is to include a cocurrent depressurization (CoD) step along with the countercurrent depressurization (CnD) step. This added step decreases the pressure in the column from the high pressure to some intermediate pressure while still producing a light product gas. In this way, some of the light inert gas is displaced from the void spaces in the column with the heavy gas that desorbs during this cocurrent depressurization step. During the subsequent CnD and LR (countercurrent purge) steps, this heavy product gas is further enriched (concentrated) in the column and recovered in the heavy product stream at a higher purity. However, depending on the intermediate pressure achieved during CoD, some of the heavy component may be lost in the light product stream causing the CO_2 recovery to decrease. Also, to avoid significant loss of the heavy product in the light product stream, typically the cycle time or the feed flow rate must be decreased with the inclusion of a CoD step (with both diminishing the throughput).

Two hundred and seventy-five (275) simulations were run to investigate the effect of the CoD step, 125 simulations in a 4-bed configuration (Figure 1c) with the intermediate pressure (P_I) fixed at 101.3 kPa and the CoD and CnD each consuming half of the cycle step time allotted for the other steps, 25 simulations in a 5-bed configuration (Figure 1b) with the intermediate pressure (PI) fixed at 101.3 kPa and the CoD and CnD each having the same cycle step time allotted for the other steps, and 125 simulations in a 4-bed configuration (again, Figure 1c) with P_I fixed at 68.9 kPa and the CoD and CnD each consuming half of the cycle step time allotted for the other steps.

Two throughputs, 14.4 and 11.5 L STP/kg/hr, were studied with these PSA cycles, as indicated in Tables 3 to 5. The lower value corresponds to the effect of adding the fifth bed to the cycle configuration to allow for all five steps to be carried out with the same cycle step time. Figure 8 compares the effect of adding the CoD step in both 4-bed and 5-bed configurations (Figures 1c and 1b, respectively) with P_I fixed at 101.3 kPa to the 4-Bed stripping PSA cycle with light reflux and no CoD step (Figure 1a). Figure 9 compares the effect of changing PI form 101.3 to 68.9 kPa in the 4-bed configuration (Figures 1c). Within each figure, five pressure ratios, five cycle step times and five purge to feed ratios were also investigated. The values of these parameters are the same as those studied in Part I and provided in Table 2, with the range provided in Table 3. The effects of these parameters can be observed from a careful examination of each figure within Figure 6; however, since the interpretation is the same as presented in Part I of this study, it is not discussed any further in this section. Tables 3, 4 and 5 respectively show the ranges of the process conditions, the corresponding ranges of the resulting performances, and the conditions that resulted in the best performance of these 4-bed and 5-bed stripping PSA cycles with light reflux and with inclusion of a CoD step.

The comparison between the original 4-bed LR cycle, the 5-bed LR cycle with CoD and CnD, and the 4-bed LR cycle with CoD and CnD shown in Figure 8 reveals only marginal but always positive effects of adding a cocurrent depressurization step. Essential no change in performance resulted, in terms of CO_2 purity and recovery, when adding the CoD step as a fifth step with its step time equal to all the other step times (5-bed configuration). However, in this case, even though for a given recovery, the purity always increased, the performance in terms of throughput actually decreased due to the addition of the fifth bed with everything else being held constant. In contrast, the change in performance, in terms of purity and recovery, was always slightly better when adding the CoD step as a fifth step with its step time equal to the CnD step time and half of that of the other step times (4-bed configuration). For example, for a given recovery, the purity always increased and in this case at the same throughput. One plausible reason for the only marginal effects observed here on the process performance when including a CoD step is associated with the value of PI not being low enough to foster significant desorption of the heavy component during the CoD step.

Hence, one of the more important variables when including a CoD step in a 4-bed stripping PSA cycle with LR is the intermediate pressure, P_I. If this intermediate pressure is too high, then throughput is diminished and recovery is lost without a significant gain in purity. If P_I is too low, then throughput is diminished with a corresponding large decrease in recovery but with a possible significant gain in purity. The most important point is that the intermediate pressure should correspond to a steeper region of the heavy component adsorption isotherm to

foster significant desorption during the CoD step.

Figure 9 shows the effect of operating at a lower intermediate pressure by comparing the same 4-bed stripping PSA cycle with light reflux and with CoD and CnD steps, but with different intermediate pressures of 101.3 and 68.9 kPa. In all cases, the lower PI caused the process performance to improve in terms of the CO_2 purity; but this improvement came at the expense of decreasing the CO_2 recovery. For example, with $\gamma = 0.5$, $t_s = 500$ s and $\pi_T = 12$, the purity increased from 64.1% to 67.8% while R decreased from 83.2% to 82.6%. This marginal improvement also came at the expense of having to use a vacuum pump to draw gas from the light product end of the column to attain a $P_I = 68.9$ kPa.

Hence, although a cocurrent depressurization step is utilized in many industrial PSA processes, it does not appear to be a viable option for improving the performance of this particular PSA process much beyond that which can be archived with the 4-bed stripping PSA process with light reflux and only a CnD step. The CoD step was not investigated any further. Instead a heavy reflux step was added to the traditional 4-step stripping PSA process with light reflux. These novel heavy reflux cycles are discussed below.

5-Step Stripping PSA Cycles with LR and or HR: Another way to improve the heavy product purity is by including a heavy reflux or cocurrent high-pressure purge or rinse step. This step, which was first patented by Tamura in 1974 and then by Sircar in 1977, takes a portion of the heavy product gas from the low-pressure column during the countercurrent depressurization step, the light reflux step or both, and uses it as high pressure purge or heavy reflux in the high-pressure column following the feed step. This heavy reflux step, while filling the column from the feed end with the heavy component, effectively purges the light component from the void spaces within the column, which is collected as light product during this step. During the subsequent CnD and or LR steps, the heavy component gas added to the column during the HR step is removed and collected as the heavy product now highly enriched in the heavy component. A HR step can be used in conjunction with a LR step, being in reality a dual reflux PSA cycle, or it can be used without a LR step, being simply a HR single reflux PSA cycle. However, like with the addition of a CoD step, to avoid significant loss of the heavy product in the light product stream, typically the cycle time or the feed flow rate must be decreased with the inclusion of a HR step (with both diminishing the throughput). Also, the addition of a HR step usually requires an additional compressor to take the low pressure gas coming from the CnD or LR step and compress it to the high pressure before being fed to the high pressure column.

One thousand, four hundred and twenty-five (1,425) simulations were run to investigate various HR PSA cycles, 500 simulations in a 5-bed configuration (Figure 1e) with the heavy reflux gas coming from the light reflux purge step (i.e., a dual reflux cycle), 500 simulations in the same bed configuration but with the adsorption and desorption mass transfer coefficients each increased by a factor of five (i.e., k = 5k), 300 simulations in a 5-bed configuration (Figure 1d) with the heavy reflux gas coming from the countercurrent depressurization step instead of the LR step (still a dual reflux cycle), and 125 simulations in a 4-bed configuration (Figure 1f) with the heavy reflux gas coming from the countercurrent depressurization gas but with no light reflux step.

Throughputs ranging from 5.8 to 34.6 L STP/kg/hr were studied with these HR PSA cycles, except for the 4-bed stripping PSA cycle with only HR, as indicated in Tables 3 to 5. A single throughput of only 7.2 L STP/kg/hr was studied in this case. Figure 10 compares the effect of five different recycle ratios (RRs) varying from 0.0 to 0.8 on the process performance of the 5-bed stripping PSA cycle with LR and HR from depressurization. The RR is defined here as the fraction of gas coming from the CnD step that is recycled as heavy reflux. Figure 11 compares the effect of five different recycle ratios (RRs) varying from 0.0 to 0.8 on the process performance of the 5-bed stripping PSA cycle with LR and HR from light reflux purge. The RR is defined here as the fraction of gas coming from the LR step that is recycled as heavy reflux. Figure 12 compares the same HR bed configuration as in Figure 11 but with the adsorption and desorption mass transfer coefficients each increased by a factor of five (i.e., k = 5k). Figure 13 compares the effect of five different recycle ratios (RRs) varying from 0.0 to 0.8 on the process performance of the 4-bed stripping PSA cycle with HR from depressurization. Within each figure, five pressure ratios and five cycle step times were also investigated. The values of these parameters are the same as those studied in Part I and provided in Table 2, with the range provided in Table 3. The effects of these parameters can be observed from a careful examination of each figure within Figures 10 to 13; however, since the interpretation is the same as presented in Part I of this study, it is not discussed any further in this section. Tables 3, 4 and 5 respectively show the ranges of the process conditions, the corresponding ranges of the resulting performances, and the conditions that resulted in the best performance of these 4-bed and 5-bed stripping PSA cycles with light and or heavy reflux (i.e., dual reflux) steps.

The results in Figure 10 for the 5-bed stripping PSA cycle with LR and HR from depressurization show very clearly that the HR step does indeed increase the CO_2 purity as the RR increases. For example, the CO_2 purity increases from 66.4% to 70.4% while the recovery decreases from 69.8% to 66.3% with the RR increasing from 0.0 to 0.8 and with θ = 17.3 L STP/hr/kg, γ = 0.5, t_s = 500 s and π_T = 12. However, the changes in the process performance with an increase in the RR were not as much as initially expected. The reason for this subtle and highly diminished effect of the HR step was due to the fact that the HR gas was taken from the CnD step. The flow rate and hence total amount of the depressurization gas available for HR was in fact quite small, which necessarily limited the amount of gas that could be used as HR to enrich the heavy product. In contrast, it was later revealed that the depressurization flow rate was approximately three to four times less than the LR flow rate. With this in mind, the effect of the HR step on the process performance should be much more pronounced when the HR gas is obtained from the LR purge step instead of the CnD step. These results are shown in Figure 11.

The results in Figure 11 for the 5-bed stripping PSA cycle with LR and HR from purge show a dramatic and positive effect of the RR on the process performance in terms of the CO_2 purity but at the expense of significantly decreasing the CO_2 recovery. For example, the CO_2 purity increases from 66.4% to 78.3% while the CO_2 recovery decreases from 69.8% to 41.7% with the RR increasing from 0.0 to 0.8 and with θ = 17.3 L STP/hr/kg, γ = 0.5, t_s = 500 s and π_T = 12. This is in stark contrast to the effects of the HR step shown in Figure 10. As just alluded to, the marked increase in CO_2 purity that resulted from the 5-bed stripping PSA cycle with HR from LR purge as compared to the same PSA cycle with HR from depressurization was caused by the larger purge flow rate (amount) compared to depressurization flow rate (amount) that allowed more CO_2 to enter the high pressure column. As more CO_2 entered the column, more

CO_2 was adsorbed leading to higher heavy product purity. However, the more CO_2 that entered the column during the HR step increased the breakthrough of CO_2 in the light product gas, causing a substantial decrease in the CO_2 recovery as the RR increased.

Nevertheless, the HR PSA cycle appears to work quite well in enriching the heavy product. For example, the 5-bed stripping PSA cycle with LR and HR from purge produced the best process performance so far among all the cycles discussed up to this point, at least in terms of CO_2 purity (78.9 %) with a reasonable throughput (11.5 L STP/kg/hr) but unfortunately with a rather low recovery (57.4 %) (Table 5 and Figure 11b). The improvement in the performance of this HR PSA cycle is even more impressive when the mass transfer coefficients are increased by a factor of five, as shown in Figure 12.

Figure 12 shows the results of the five times higher mass transfer coefficients for the 5-bed stripping PSA cycle with LR and HR from purge. A detailed comparison between the results in Figures 11 and 12 reveals that for a given throughput both the CO_2 purity and CO_2 recovery increased substantially with an increase in the mass transfer coefficients. This marked improvement is also revealed in Table 5, with the best PSA process performance coming from this cycle. For example, a CO_2 purity of 90.3% was obtained at a CO_2 recovery of 73.6% with a relatively high throughput of 34.6 L STP/kg/kr and with RR=0.8, $\pi_T = 12$, $\gamma = 0.5$ and $t_s = 500$ s. These results further emphasize the importance of determining accurate mass transfer coefficients for the CO_2-HTlc adsorbate-adsorbent system.

The final PSA cycle evaluated in this study was a 4-bed stripping PSA cycle with heavy reflux from depressurization (because no light reflux step was included). This cycle was worth evaluating because by eliminating the light reflux step only 4 beds were needed and more importantly dilution of the heavy product gas would be minimized. The results are shown in Figure 13 for three throughputs ranging from 5.8 to 11.2 to 17.3 L STP/kg/hr. In general, a comparison of Figures 10 and 13 reveals that under similar conditions, elimination of the LR step resulted in slight decreases in the CO_2 purity and marked decreases in the CO_2 recovery. The recoveries were greatly reduced because without LR it was very difficult to effect substantial regeneration of the adsorbent during the cycle. Since the adsorbent was not very well regenerated, breakthrough of CO_2 into the light product gas was more prevalent thereby reducing the CO_2 recovery. For $\theta = 17.3$ L STP/hr/kg, RR=0.8, $\gamma = 0.5$, $t_s = 500$ s and $\pi_T = 12$, the recovery for the 5-bed process (Figure 10) was 66.3% while it was 4.4% for the 4-bed process Figure 13). Moreover, the purity for the 4-bed process without LR was also less than that for the 5-bed process. The purity for the 5-bed process was 70.4% (Figure 10) while it was 69.4% for the 4-bed process (Figure 13). Apparently, when the heavy reflux comes from the depressurization step, as it did in both of these cycles, the CO_2 purity in the heavy product stream improves during and because of the LR step, which also improves the recovery, as discussed. The best performance for this 4-bed stripping PSA cycle with heavy reflux from depressurization was the worst of all the cycles studied with a CO_2 purity of 55.9% at a CO_2 recovery of only 26.4% and a low throughput of only 7.2 L STP/kg/hr.

Conclusions

Overall, the results of this study suggest that a dual reflux (LR and HR) PSA process configuration provides the best performance. A careful examination of the results in Table 5 provides clear evidence of this statement about the use of a HR step, but only when combined with a LR step. The results in Figures 4 also show that the heavy reflux concept far outperforms the light reflux concept. In terms of CO_2 purity, for example, the dual reflux, 5-bed stripping PSA cycle with LR and HR from purge performed the best, especially when the mass transfer coefficients were increased by a factor of five. The next best PSA cycle was the dual reflux, 5-bed stripping PSA cycle with LR and HR from depressurization. In general, the single reflux, 4-bed or 5-bed stripping PSA cycles with LR or HR did not perform that well in terms of producing a heavy product steam enriched in CO_2. This was the case even when a cocurrent depressurization step was included with the LR cycle or even when the mass transfer coefficients were increased by a factor of five for the 4-bed stripping PSA cycle with LR. The question that will be addressed over the next three years is how to improve the performance of this dual reflux process in terms of increasing the purity, recovery and throughput through creative PSA cycle design configuration based on some novel cycles in the literature and some new proprietary cycles.

The results of this study also suggest that the mass transfer plays a key role in improving the PSA process performance. The effect of the mass transfer coefficient was clearly revealed in Table 5 and by comparing the graphs in Figures 6 and 7 for the 4-bed stripping PSA cycles with LR and Figures 11 and 12 for the 4-bed stripping PSA cycles with LR and HR from purge. An increase in the mass transfer coefficient by a factor of five increased the recovery substantially while also increasing the purity modestly. The question that will be addressed over the next three years is how to accurately measure the mass transfer properties of the K-promoted HTlc adsorbent, because the results in the literature are controversial. The original work by Hufton et al (1999) with this material suggests very fast time constants, which contradicts the work by Ding and Alpay (2001) and the lower values used in most of these simulations.

References

Baksh, M.S.A., A. Kapoor, and R.T. Yang, "A New Composite Sorbent for Methane-Nitrogen Separation by Adsorption," *Sep. Sci. Technol.*, **25**, 845-868 (1990).

Caldeira, K., A.K. Jain, and M.I. Hoffert, "Climate Sensitivity Uncertainty and the Need for Energy Without CO_2 Emission," *Science*, **299**, 2052-2054 (2003).

Cen, P.L. and R.T. Yang, "Separation of Binary Gas Mixture into Two High-Purity Products by a New Pressure Swing Adsorption Cycle," *Sep. Sci. Technol.*, **21**, 845-864 (1986).

Ding, Y. and E. Alpay, "Equilibria and Kinetics of CO_2 Adsorption on Hydrotalcite Adsorbent," *Chem. Eng. Sci.*, **55**, 3461-3474 (2000).

Ding, Y. and E. Alpay, "High Temperature Recovery of CO_2 from Flue Gases Using Hydrotalcite Adsorbent," *Trans IChemE*, **79**, 45-51 (2001).

Kratz, W.C., D.L. Rarig, and J.M. Pietrantonio, "Hydrogen and Carbon Dioxide Coproduction from SMR Offgas by Pressure Swing Adsorption," *AIChE Symp. Ser.*, **84**, 36-43 (1988).

Liu, Y. and J.A. Ritter, "Pressure Swing Adsorption-Solvent Vapor Recovery: Process Dynamics and Parametric Study," *Ind. Eng. Chem. Res.*, **35**, 2299-2312 (1996).

Liu, Y., C.E. Holland, J.A. Ritter, "Solvent Vapor Recovery by Pressure Swing Adsorption. I. Experimental Study on the Transient and Periodic Dynamics of the Butane-Activated Carbon System," *Sep. Sci. Technol.*, **33**, 2311-2334 (1998).

Liu, Y., C.E. Holland, J.A. Ritter, "Solvent Vapor Recovery by Pressure Swing Adsorption. III. Comparison of Simulation with Experiment for the Butane-Activated Carbon System," *Sep. Sci. Technol.*, **34**, 1545-1576 (1999).

Liu, Y., J.A. Ritter, B.K. Kaul, "Simulation of Gasoline Vapor Recovery by Pressure Swing Adsorption," *Sep. Purif. Technol.*, **20**, 111-127 (2000).

Na, B., H. Lee, K. Koo, H.K. Song, "Effect of Rinse and Recycle Methods on the Pressure Swing Adsorption Process to Recover CO_2 from Power Plant Flue Gas Using Activated Carbon," *Ind. Eng. Chem. Res.*, **41**, 5498-5503 (2002).

Olajossy, A., A. Gawdzik, Z. Budner, J. Dula, "Methane Separation from Coal Mine Methane Gas by Vacuum Pressure Swing Adsorption," *Trans. IChemE.*, 81, 474-482 (2003).

Reynolds, S.P., A.D. Ebner, and J.A. Ritter, "New Pressure Swing Adsorption Cycles for Carbon Dioxide Sequestration," *Adsorption*, **11**, 531-536 (2005).

Ruthven, D.M., S. Farooq, and K.S. Knaebel, *Pressure Swing Adsorption*, VCH Publishers, Inc., New York (1994).

Sikavitsas, V.I., R.T. Yang, M.A. Burns, and E.J. Langenmayr, "Magnetically Stabilized Fluidized Bed for Gas Separations: Olefin-Paraffin Separations by π-Complexation," *Ind. Eng. Chem. Res.*, **34**, 2873-2880 (1995).

Sircar, S. and J.W. Zondlo, U.S. Patent 4,013,429 (1977).

Subramanian, D. and J.A. Ritter, "Equilibrium Theory for Binary Solvent Vapor Recovery by Pressure Swing Adsorption: Analytical Solution for Process Performance," *Chem. Eng. Sci.*, **52**, 3147-3160 (1997).

Suh, S. and P.C. Wankat, "A New Pressure Swing Adsorption Process for High Enrichment and Recovery," *Chem. Eng. Sci..*, **44**, 567-574 (1989).

Tamura, T., U.S. Patent 3,797,201 (1974).

Yong, Z., V. Mata, A.E. Rodrigues, "Adsorption of Carbon Dioxide on Basic Alumina at High Temperatures," *J. Chem. Eng. Data*, **45**, 1093-1095 (2000).

Yong, Z., V. Mata, A.E. Rodrigues, "Adsorption of Carbon Dioxide onto Hydrotalcite-like

Compounds (HTlcs) at High Temperatures," *Ind. Eng. Chem. Res.*, **40**, 204-209 (2001).
Yong, Z., V. Mata, A.E. Rodrigues, "Adsorption of Carbon Dioxide at High Temperature – A Review," *Separ. Purif. Technol.*, **26**, 195-205 (2002).

Nomenclature

A_i	gas/adsorbed phase heat capacity parameter (kJ/mol/K)
B_i	gas/adsorbed phase heat capacity parameter (kJ/mol/K^2)
B_i^0	adsorption isotherm parameter (K)
b_i	adsorption isotherm parameter (kPa^{-1})
b_i^0	adsorption isotherm parameter (kPa^{-1})
C_i	gas/adsorbed phase heat capacity parameter (kJ/mol/K^3)
$C_{P,g}$	gas phase heat capacity (kJ/mol/K)
$C_{P,g,i}$	gas phase heat capacity of component i (kJ/mol/K)
$C_{P,p}$	heat capacity of adsorbent particle (kJ/mol/K)
D_i	gas/adsorbed phase heat capacity parameter (kJ/mol/K^4)
h	overall heat transfer coefficient (kW/m^2/K)
ΔH_i	isosteric heat of adsorption of component i (kJ/mol)
k_i	mass transfer coefficient (s^{-1})
MW_i	molecular weight of component i (kg/mol)
P	pressure (kPa)
P_H	high pressure (kPa)
P_L	low pressure (kPa)
q_i	loading of component i (mol/kg)
q_i^*	equilibrium loading of component i (mol/kg)
q_i^s	saturation loading of component i (mol/kg)
r_b	radius of the bed (m)
R	universal gas constant (kPa·m3/mol/K) or recovery
S_i	defined by equation 3
t	time (s)
t_c	cycle time (s)
t_s	cycle step time (s)
T	temperature (K)
T_o	wall temperature (K)
T_f	feed temperature (K)
u	interstitial velocity (m/s)
u_f	feed interstitial velocity (m/s)
u_{LR}	light reflux interstitial velocity (m/s)
u_{HR}	heavy reflux interstitial velocity (m/s)
y_i	mole fraction of component i
z	column position (m)

Greek Letters

ε	bed porosity
γ	light product purge to feed ratio
χ	particle porosity
φ	gas phase capacitance inside the pore
$\rho_{a,i}$	adsorbed phase density of component i (kg/m^3)
ρ_p	adsorbent particle density (kg/m^3)

θ feed throughput (L STP/hr/kg)
π_T high to low pressure ratio

Table 1. Bed characteristics, gas phase species and HTlc adsorbent transport and thermodynamic properties.

Bed, HTlc Adsorbent and Process Characteristics	
Bed Length (L)	0.2724 m
Bed Radius (r_b)	0.0387 m
Bed Porosity (ε)	0.48
Adsorbent Particle Radius (r_p)	0.001375 m
Adsorbent Particle Density (ρ_p)	1563 kg/m^3
Adsorbent Particle Heat Capacity ($C_{P,p}$)	0.850 kJ/kg/K
CO_2-HTlc Isosteric Heat of Adsorption (ΔH_i)	9.29 kJ/mol
Heat Transfer Coefficient (h)	0.00067 kW/m^2/K
CO_2-HTlc Mass Transfer Coefficient: ads (k_a), des (k_d)	0.0058 s^{-1}, 0.0006 s^{-1}
Feed Mole Fractions: CO_2, N_2, and H_2O	0.15, 0.75 and 0.10
Feed (T_f) and Wall Temperature (T_o)	575 K
Adsorption Isotherm Coefficients for CO_2	
$q_{i,1}^s$ for CO_2 (mol/kg/K)	-1.5277E-3
$q_{i,2}^s$ for CO_2 (mol/kg)	1.7155
b_i^0 for CO_2 (kPa^{-1})	0.0203
B_i^0 for CO_2 (K)	1118.1
Gas and Adsorbed Heat Capacity Coefficients for CO_2, N_2 and H_2O	
A_i for CO_2, N_2, and H_2O (kJ/mol/K)	1.9795E-2, 3.1123E-2, 3.2221E-2
B_i for CO_2, N_2, and H_2O (kJ/mol/K^2)	7.3437E-5, -1.3553E-5, 1.9217E-6
C_i for CO_2, N_2, and H_2O (kJ/mol/K^3)	-5.6019E-8, 2.6772E-8, 1.0548E-8
D_i for CO_2, N_2, and H_2O (kJ/mol/K^4)	1.7153E-11, 1.1671E-11, -3.5930E-12

Table 2. Fixed and varied process parameters studied in Part I. The values underlined indicate base case conditions.

High Pressure (P_H)	137.9 kPa
Pressure Ratio ($\pi_T = P_H/P_L$)	4, 6, <u>8</u>, 10, 12
Feed Flow Rate (V_f)	1.0 L STP/min
Throughput (θ)	14.4 L STP/hr/kg
Purge to Feed Ratio (γ)	0.50, <u>0.75</u>, 1.00, 1.25, 1.50
Cycle Step Time (t_s)	100 s, 200 s, <u>300 s</u>, 400 s, 500 s
Total Cycle Time (t_c)	400 s, 800 s, 1200 s, 1600 s, 2000 s

Table 3. Range of process conditions studied for each of the six PSA cycle configurations.

Cycle Description	Throughput θ (L STP/hr/kg)	Pressure Ratio[A] (P_H/P_L)	Cycle Time[B] t_c (s)	Purge-to-Feed Ratio γ
4-Bed Stripping PSA Cycle with LR	3.6 – 43.2	4 – 12	400 – 2000	0.5 – 1.5
4-Bed Stripping PSA Cycle with LR: k = 5k	7.2 – 43.2	4 – 12	400 – 2000	0.5
4-Bed Stripping PSA Cycle with LR and CoD and CnD ($t_{co} = t_{cn} = 0.5t_s$; P_I = 101.3 kPa)	14.4	4 – 12	400 – 2000	0.5 – 1.5
5-Bed Stripping PSA Cycle with LR and Co and CnD ($t_{co} = t_{cn} = t_s$ P_I = 101.3 kPa)	11.5	4 – 12	500 – 2500	0.5
4-Bed Stripping PSA Cycle with LR and CoD and CnD ($t_{co} = t_{cn} = 0.5t_s$; P_I = 68.9 kPa)	14.4	4 – 12	400 – 2000	0.5 – 1.5
5-Bed Stripping PSA Cycle with LR and HR from Purge	5.8 – 34.6	4 – 12	500 – 2500	0.5
5-Bed Stripping PSA Cycle with LR and HR from Purge: k = 5k	5.8 – 34.6	4 – 12	500 – 2500	0.5
5-Bed Stripping PSA Cycle with LR and HR from Depressurization	5.8 – 17.3	4 – 12	500 – 2500	0.5
4-Bed Stripping PSA Cycle with HR from Depressurization	7.2	4 – 12	400 – 2000	0.5

[A] P_H = 137.9 kPa

[B] All step times t_s were equal in length except for the 4-Bed Stripping PSA Cycle with LR and CoD and CnD where $t_{co} = t_{cn} = 0.5t_s$.

Table 4. Range of performances achieved in terms of feed throughput, and CO_2 purity and recovery for a given PSA cycle configuration and the range of process conditions studied.

Cycle Configuration	Throughput (L STP/hr/kg)	CO_2 Purity* (%)	CO_2 Recovery* (%)	Number of Simulations
4-Bed Stripping PSA Cycle with LR	3.6 – 43.2	12.8 – 66.4 (100) (69.8)	45.5 – 100 (34.7) (49.4)	1025
4-Bed Stripping PSA Cycle with LR: k = 5k	7.2 – 43.2	37.2 – 73.5 (98.5) (89.2)	76.7 – 100 (47.2) (64.2)	125
4-Bed Stripping PSA Cycle with LR and CoD and CnD ($t_{co} = t_{cn} = 0.5t_s$; P_I = 101.3 kPa)	14.4	23.6 – 64.1 (98.9) (83.2)	59.9 – 100 (39.7) (43.0)	125
5-Bed Stripping PSA Cycle with LR and Co and CnD ($t_{co} = t_{cn} = t_s$ P_I = 101.3 kPa)	11.5	33.6 – 64.4 (76.3) (84.2)	60.4 – 97.3 (39.9) (43.5)	25
4-Bed Stripping PSA Cycle with LR and CoD and CnD ($t_{co} = t_{cn} = 0.5t_s$; P_I = 68.9 kPa)	14.4	25.6 – 67.8 (97.2) (82.6)	58.5 – 100 (41.1) (43.2)	125
5-Bed Stripping PSA Cycle with LR and HR from Purge	5.8 – 34.6	36.6 – 78.9 (87.2) (57.4)	22.6 – 98.0 (52.8) (38.9)	500
5-Bed Stripping PSA Cycle with LR and HR from Purge: k = 5k	5.8 – 34.6	41.1 – 90.3 (100) (73.6)	52.2 – 100 (71.1) (66.8)	500
5-Bed Stripping PSA Cycle with LR and HR from Depressurization	5.8 – 17.3	36.9 – 74.1 (87.9) (94.5)	48.8 – 98.8 (39.2) (54.8)	300
4-Bed Stripping PSA Cycle with HR from Depressurization	7.2	34.7 – 55.9 (37.8) (26.4)	10.9 – 70.5 (41.1) (40.7)	125

* The values in parentheses correspond to the highest CO_2 recovery achieved for the highest and lowest CO_2 purity, and the highest CO_2 purity achieved for the highest and lowest CO_2 recovery.

Table 5. Best performance based on highest CO_2 purity obtained for a given PSA cycle configuration and set of corresponding conditions.

Cycle Configuration	Throughput (L STP/hr/kg)	Pressure Ratio[A] (P_H/P_L)	Cycle Time[B] t_c (s)	CO_2 Purity (%)	CO_2 Recovery (%)
4-Bed Stripping PSA Cycle with LR	21.6	12	2000	66.4	69.8
4-Bed Stripping PSA Cycle with LR: k = 5k	43.2	12	2000	73.5	89.2
4-Bed Stripping PSA Cycle with LR and CoD and CnD ($t_{co} = t_{cn} = 0.5t_s$; P_I = 101.3 kPa)	14.4	12	2000	64.1	83.2
5-Bed Stripping PSA Cycle with LR and Co and CnD ($t_{co} = t_{cn} = t_s$, P_I = 101.3 kPa)	11.5	12	2500	64.4	84.2
4-Bed Stripping PSA Cycle with LR and CoD and CnD ($t_{co} = t_{cn} = 0.5t_s$; P_I = 68.9 kPa)	14.4	12	2000	67.8	82.6
5-Bed Stripping PSA Cycle with LR and HR from Purge	11.5	12	2500	78.9	57.4
5-Bed Stripping PSA Cycle with LR and HR from Purge: k = 5k	34.6	12	2500	90.3	73.6
5-Bed Stripping PSA Cycle with LR and HR from Depressurization	5.8	12	2500	74.1	94.5
4-Bed Stripping PSA Cycle with HR from Depressurization	7.2	10	2000	55.9	26.4

[A] P_H = 137.9 kPa

[B] All step times t_s were equal in length except for the 4-Bed Stripping PSA Cycle with LR and CoD and CnD where $t_{co} = t_{cn} = 0.5t_s$.

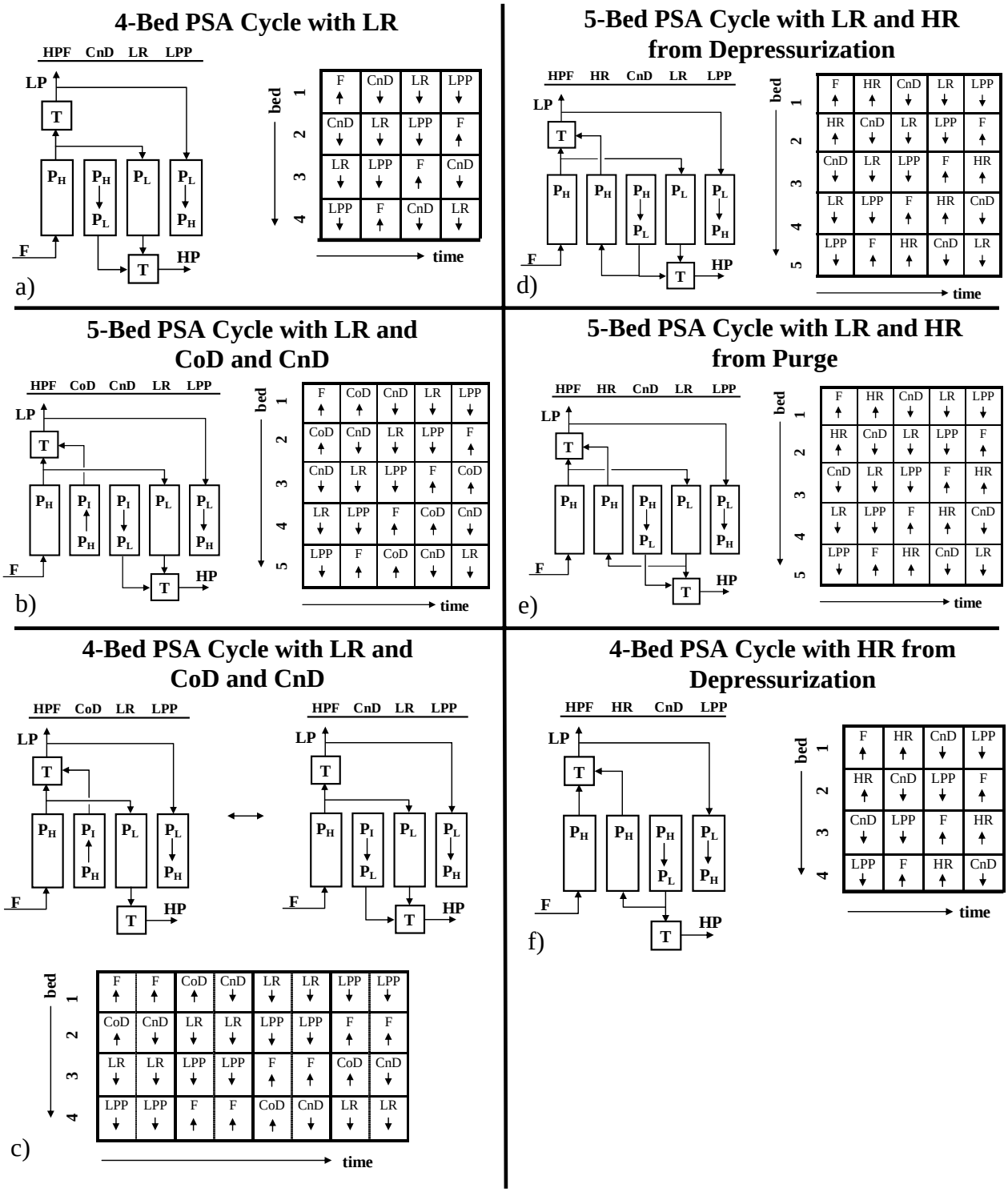

Figure 1. Schematics of the various stripping PSA cycles analyzed for high temperature CO_2 capture and concentration with the CO_2 selective K-promoted HTlc adsorbent. F = feed; CoD = cocurrent depressurization; CnD = countercurrent depressurization; LR = light reflux; HR = heavy reflux; LPP = light product pressurization; P_L = low pressure; P_H = high pressure; P_I = intermediate pressure; LP = light product; HP = heavy product; T = tank.

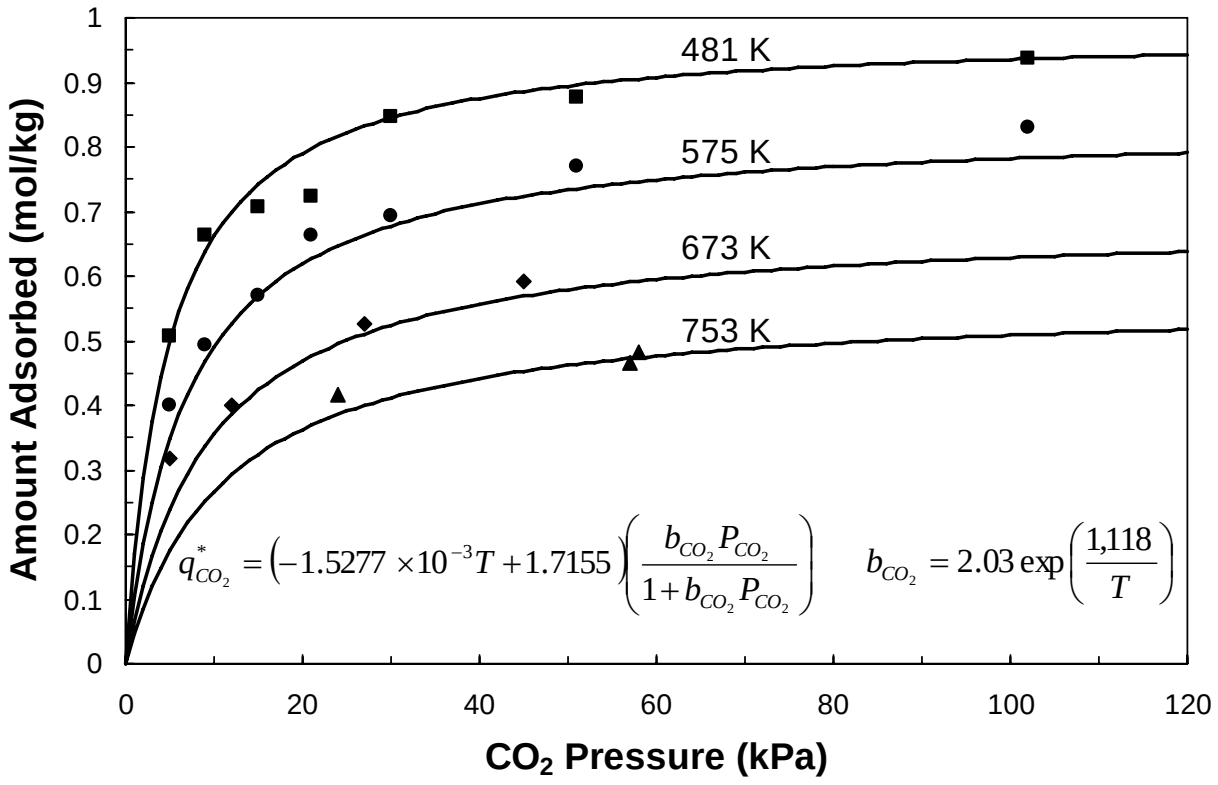

Figure 2. CO_2 adsorption isotherms for K-promoted HTlc (Ding and Alpay , 2000; 2001). Symbols: experiment; lines: model.

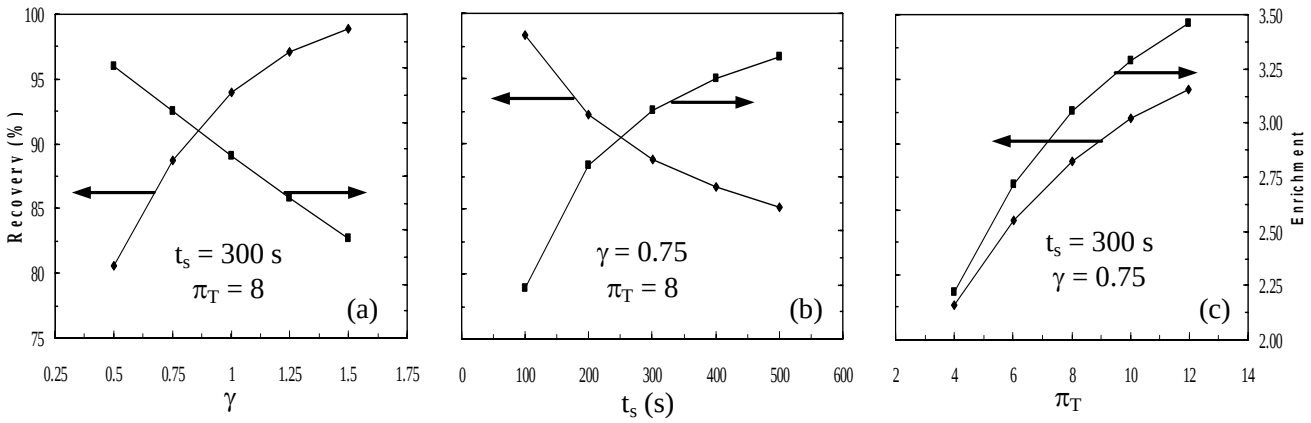

Figure 3. 4-Bed stripping PSA cycle with light reflux: Effect of the (a) purge to feed ratio (γ), (b) cycle step time (t_i), and (c) pressure ratio (π_T) on the process performance in terms of the CO_2 recovery (R) and CO_2 enrichment (E). Base case conditions used for the non-varying parameters. The throughput θ = 14.4 L STP/hr/kg.

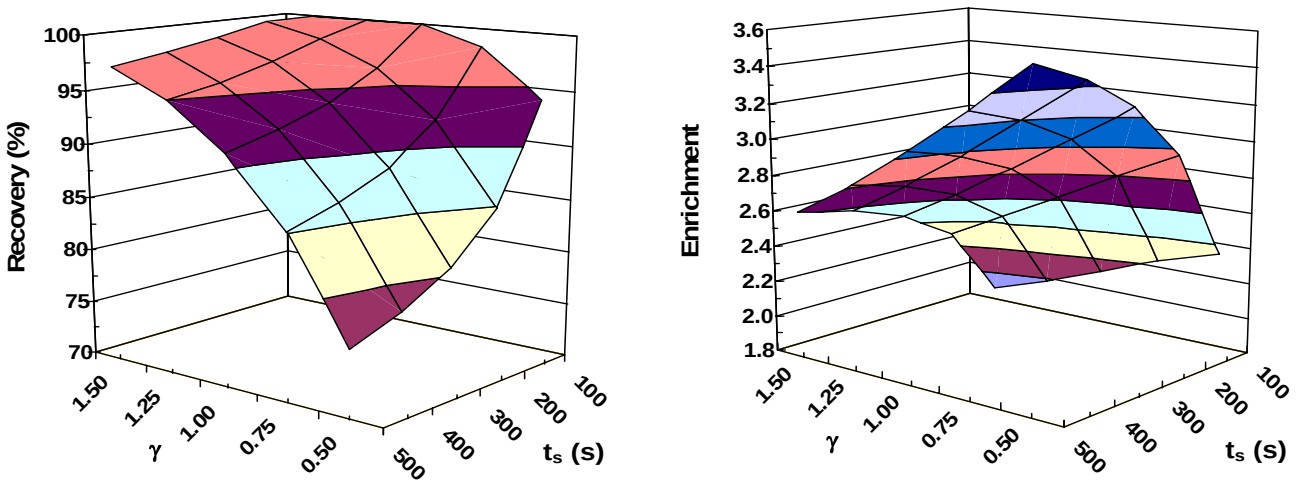

Figure 4. 4-Bed stripping PSA cycle with light reflux: Effect of the purge to feed ratio (γ) and cycle step time (t_s) on the process performance in terms of the (a) CO_2 recovery (R) and (b) CO_2 enrichment (E). Results from 25 simulations are shown with $\pi_T = 8$ and $\theta = 14.4$ L STP/hr/kg.

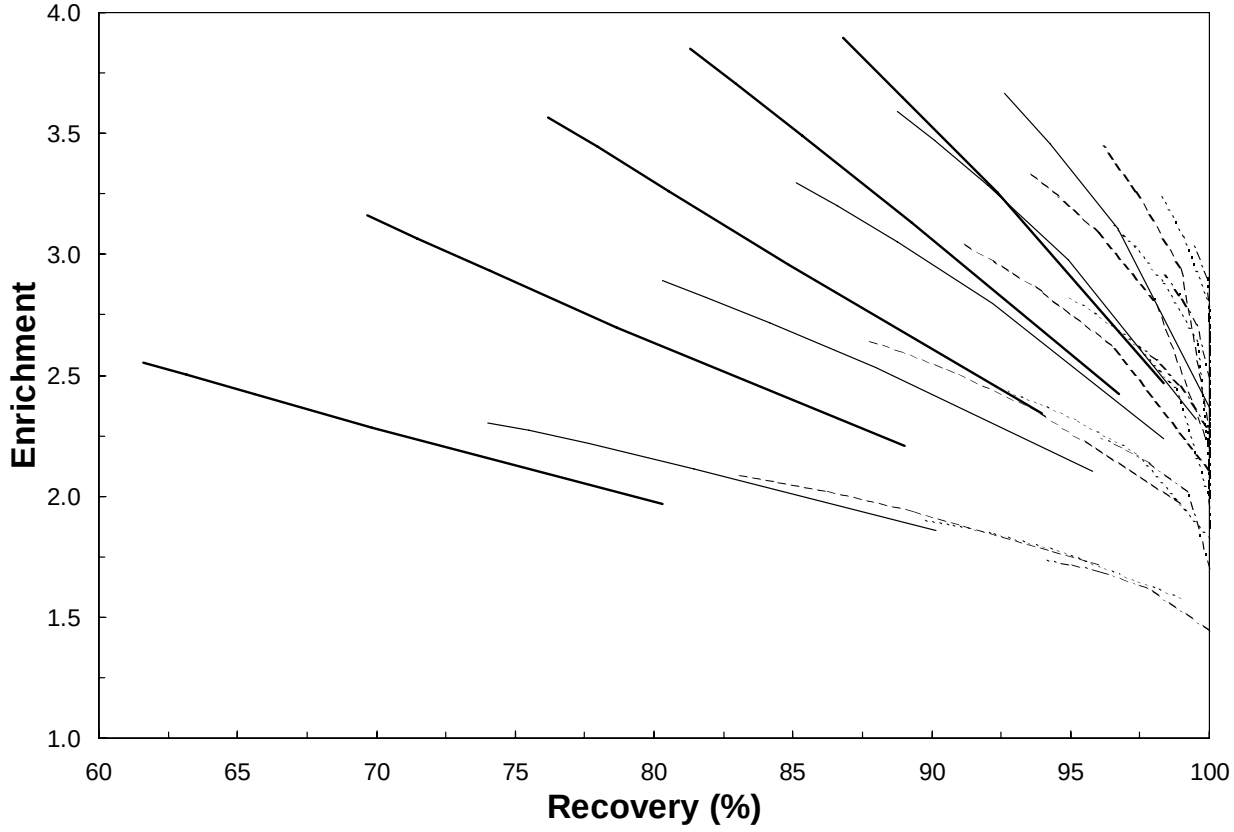

Figure 5. Comparison of performance curves for the 4-bed stripping PSA cycle with light reflux for θ = 14.4 L STP/hr/kg) and γ = 0.50 (bold line), 0.75 (thin line), 1.00 (dashed line), 1.25 (dotted line), and 1.5 (dot-and-dash). Each line corresponds to five runs with t_s increasing from right to left. Each family of lines of constant γ corresponds to π_T increasing as their fan spreads from left to right.

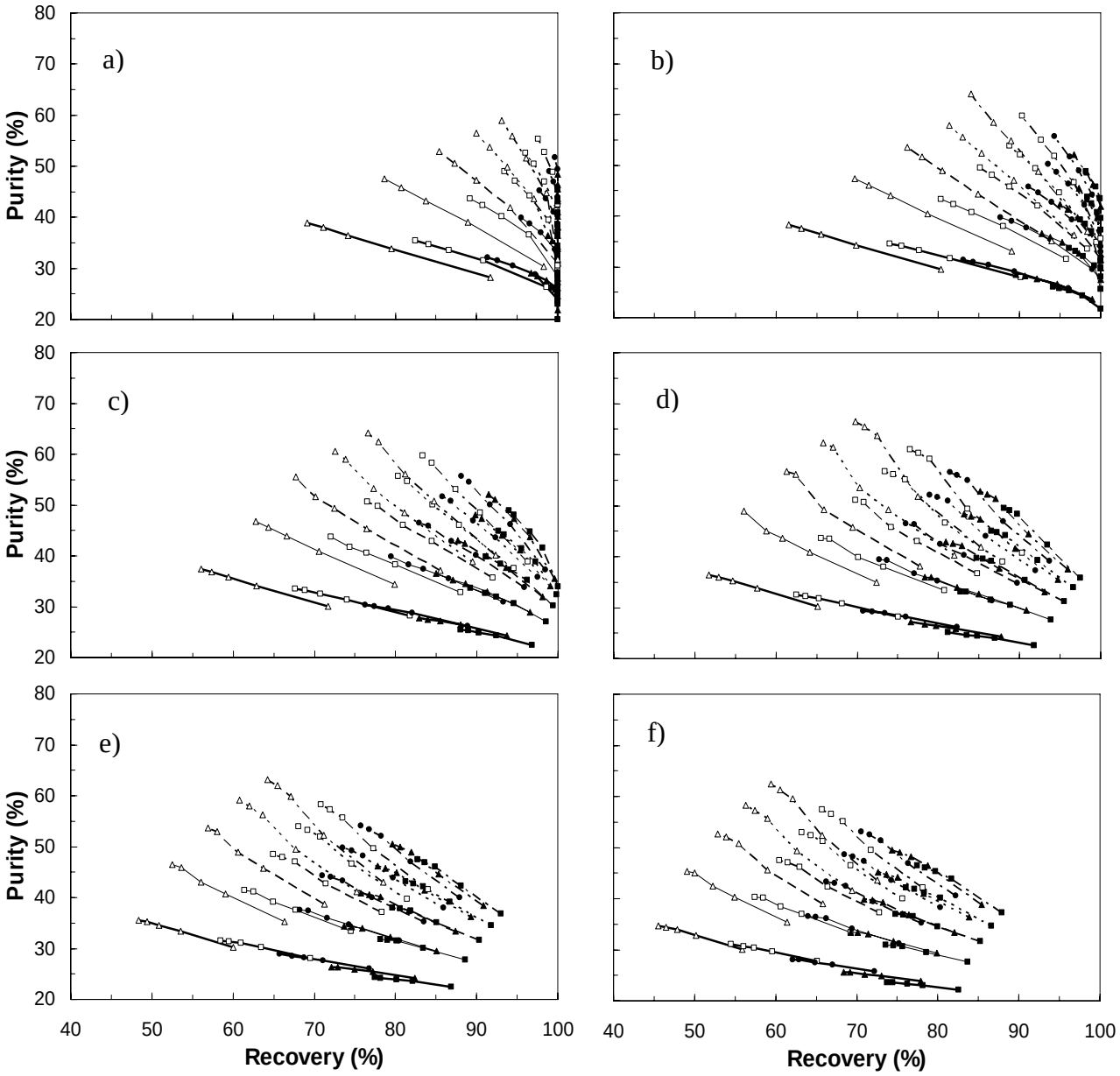

Figure 6. Comparison of performance curves for the 4-bed stripping PSA cycle with light reflux for θ = a) 10.8 L STP/hr/kg, b) 14.4 L STP/hr/kg, c) 18.0 L STP/hr/kg, d) 21.6 L STP/hr/kg, e) 25.2 L STP/hr/kg and f) 28.8 L STP/hr/kg. Each line corresponds to five runs with t_s increasing from right to left. Lines: bold – $\pi_T = 4$; thin – $\pi_T = 6$; dashed – $\pi_T = 8$; dotted – $\pi_T = 10$; dot-and-dash – $\pi_T = 12$. Symbols: filled squares – $\gamma = 1.50$; filled triangles – $\gamma = 1.25$; filled circles – $\gamma = 1.00$; empty squares – $\gamma = 0.75$; empty triangles – $\gamma = 0.50$.

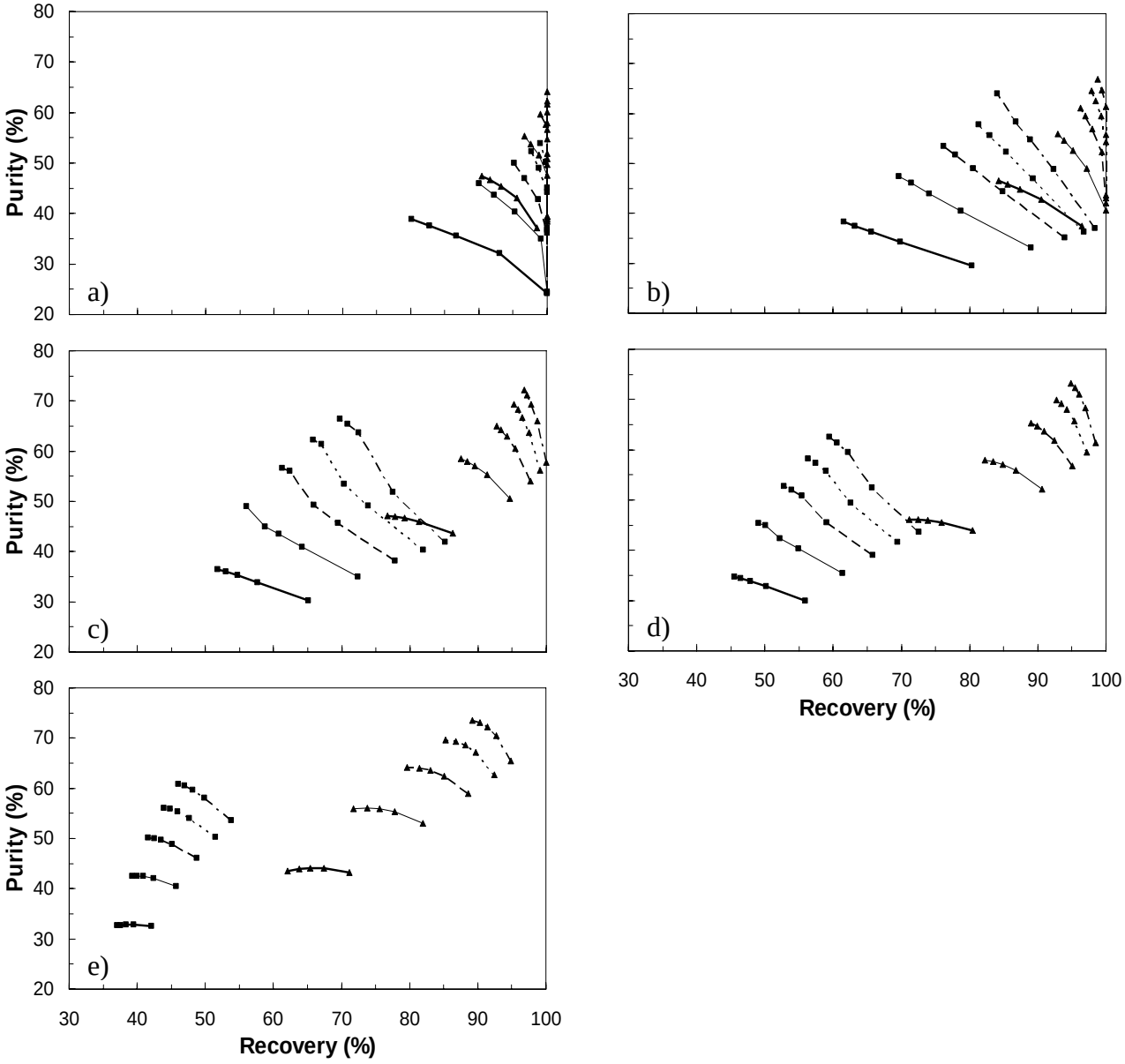

Figure 7. Comparison of performance curves obtained by increasing both the adsorption and desorption mass transfer coefficients by factors of five for the 4-bed stripping PSA cycle with light reflux for γ = 0.5 and θ = a) θ = 7.2 L STP/hr/kg, b) 14.4 L STP/hr/kg, c) 21.6 L STP/hr/kg, d) 28.8 L STP/hr/kg and e) 43.2 L STP/hr/kg. Each line corresponds to five runs with t_s increasing from right to left. Lines: bold – π_T = 4; thin – π_T = 6; dashed – π_T = 8; dotted – π_T = 10; dot-and-dash – π_T = 12. Symbols: filled squares – original mass transfer coefficients (Table 1; filled triangles – five times original mass transfer coefficients (k = 5 k).

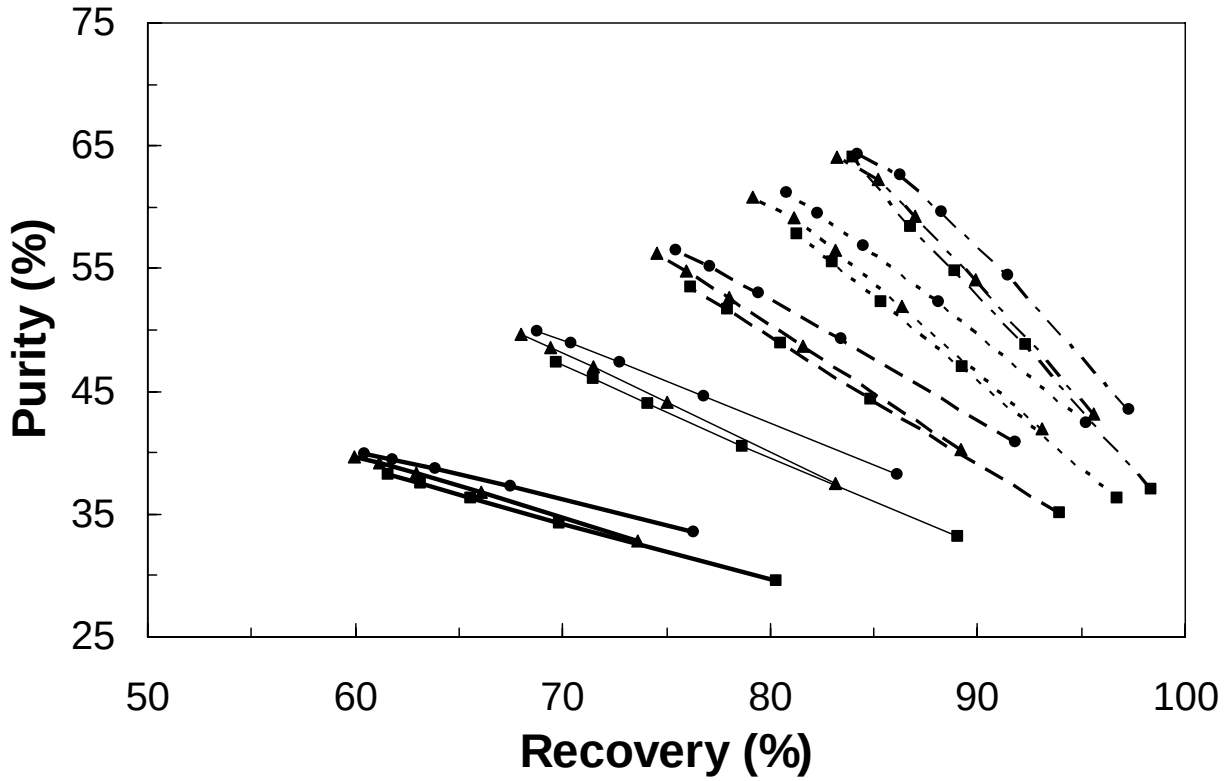

Figure 8. Comparison of performance curves for 4-bed and 5-bed stripping PSA cycles with LR and with and without CoD and CnD for $\gamma = 0.5$ and $\theta = 14.4$ L STP/hr/kg for the 4-bed LR cycle, $\theta = 14.4$ L STP/hr/kg and $P_I = 101.3$ kPa for the 4-bed LR with CoD and CnD ($t_{co} = t_{cn} = 0.5t_s$), and $\theta = 11.5$ and $P_I = 101.3$ kPa for the 5-bed LR with CoD and CnD ($t_{co} = t_{cn} = t_s$). Each line corresponds to five runs with t_s increasing from right to left. Lines: bold – $\pi_T = 4$; thin – $\pi_T = 6$; dashed – $\pi_T = 8$; dotted – $\pi_T = 10$; dot-and-dash – $\pi_T = 12$. Symbols: filled squares – 4-bed LR; filled triangles – 5-bed LR with CoD and CnD; filled circles – 4-bed LR with CoD and CnD.

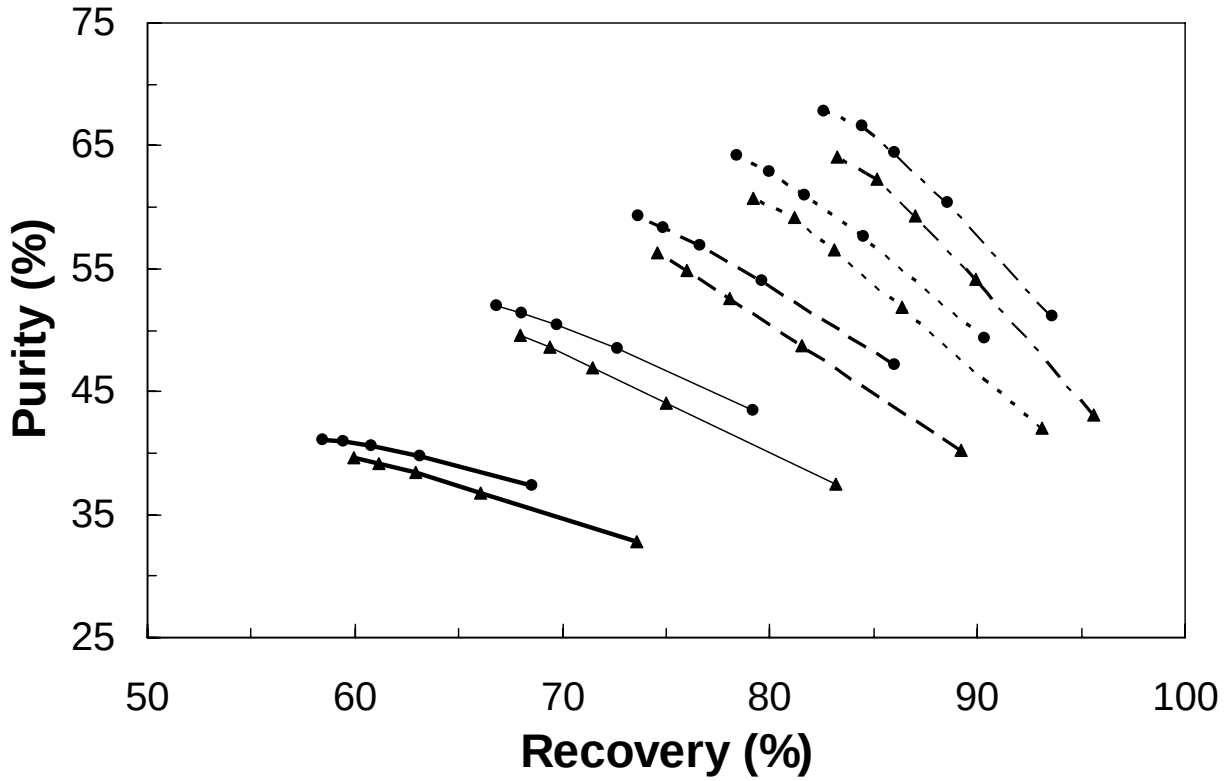

Figure 9. Comparison of performance curves with different intermediate pressures (P_I) for 4-bed stripping PSA cycles with LR and CoD and CnD for $\gamma = 0.5$ and $\theta = 14.4$ L STP/hr/kg. Each line corresponds to five runs with t_s increasing from right to left. Lines: bold – $\pi_T = 4$; thin – $\pi_T = 6$; dashed – $\pi_T = 8$; dotted – $\pi_T = 10$; dot-and-dash – $\pi_T = 12$. Symbols: filled triangles – $P_I = 101.3$ kPa; filled circles – $P_I = 68.9$ kPa.

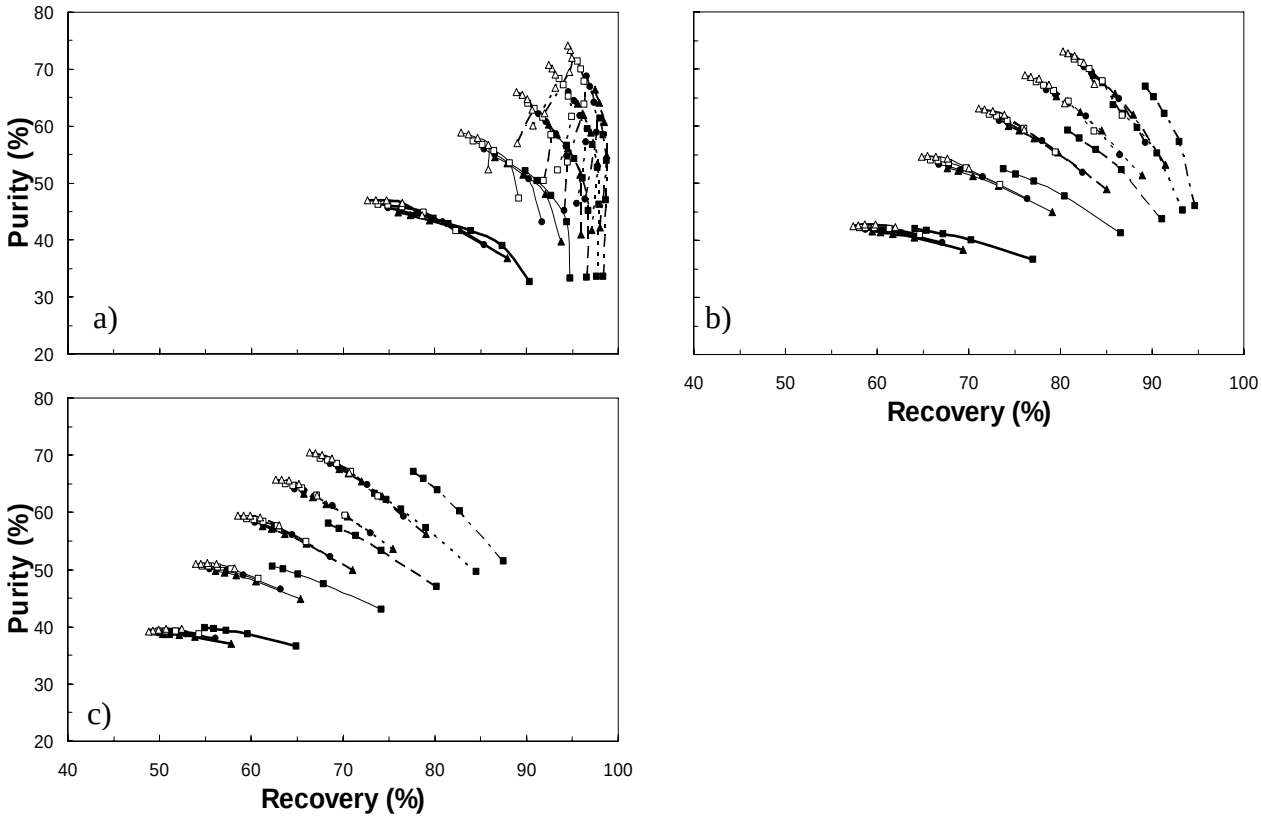

Figure 10. Comparison of performance curves for the 5-bed stripping PSA cycle with LR and HR from depressurization for γ = 0.5 and θ = a) 5.8 L STP/hr/kg, b) 11.2 L STP/hr/kg and c) 17.3 L STP/hr/kg. Each line corresponds to five runs with t_s increasing from right to left. Lines: bold – π_T = 4; thin – π_T = 6; dashed – π_T = 8; dotted – π_T = 10; dot-and-dash – π_T = 12. Symbols: filled squares – RR = 0.0; filled triangles – RR = 0.2; filled circles – RR = 0.4; empty squares – RR = 0.6; empty triangles – RR = 0.8.

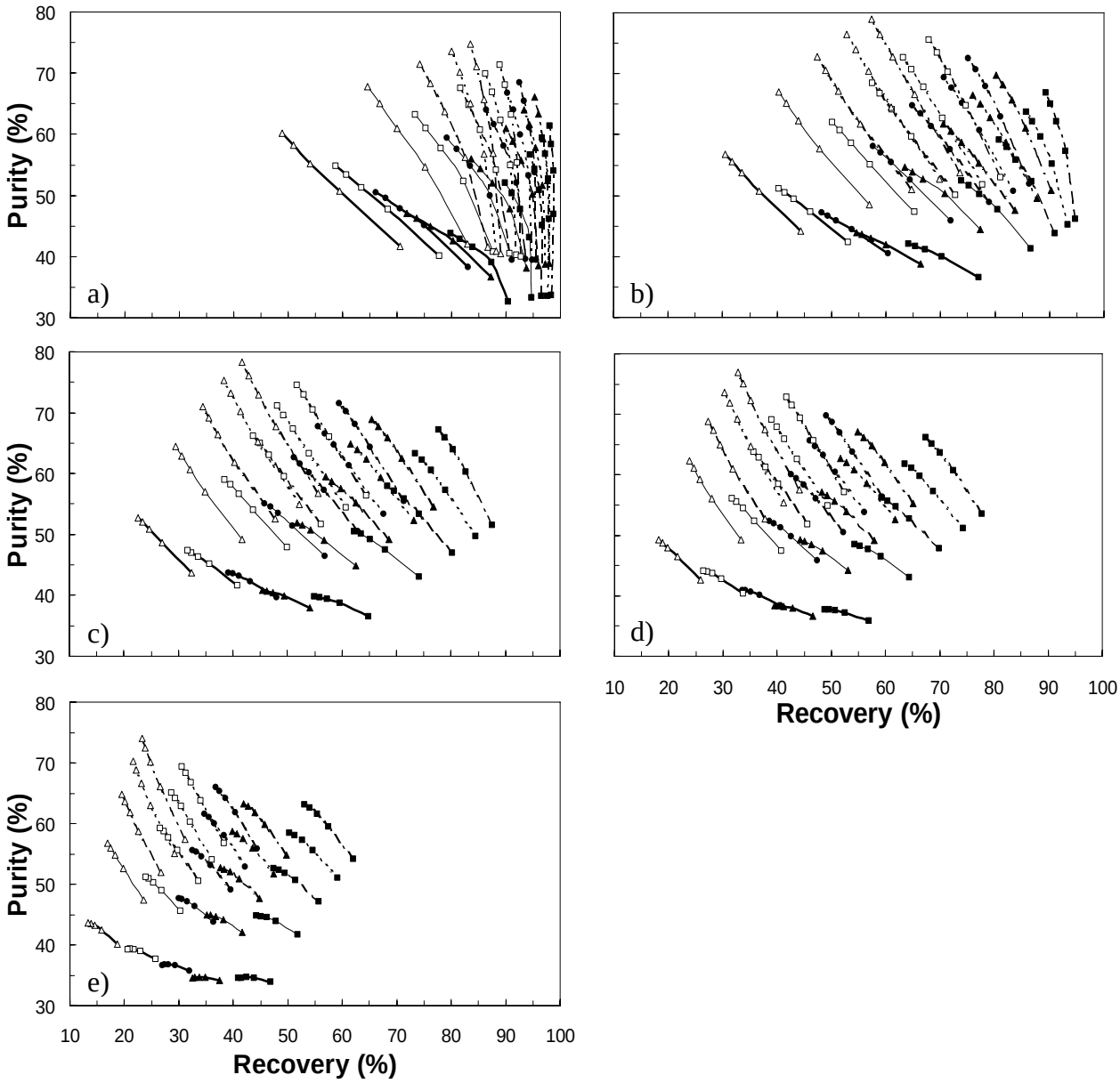

Figure 11. Comparison of performance curves for the 5-bed stripping PSA cycle with LR and HR from purge for $\gamma = 0.5$ and θ = a) 5.8 L STP/hr/kg, b) 11.2 L STP/hr/kg, c) 17.3 L STP/hr/kg, d) 23.1 L STP/hr/kg and e) 34.6 L STP/hr/kg. Each line corresponds to five runs with t_s increasing from right to left. Lines: bold – $\pi_T = 4$; thin – $\pi_T = 6$; dashed – $\pi_T = 8$; dotted – $\pi_T = 10$; dot-and-dash – $\pi_T = 12$. Symbols: filled squares – RR = 0.0; filled triangles – RR = 0.2; filled circles – RR = 0.4; empty squares – RR = 0.6; empty triangles – RR = 0.8.

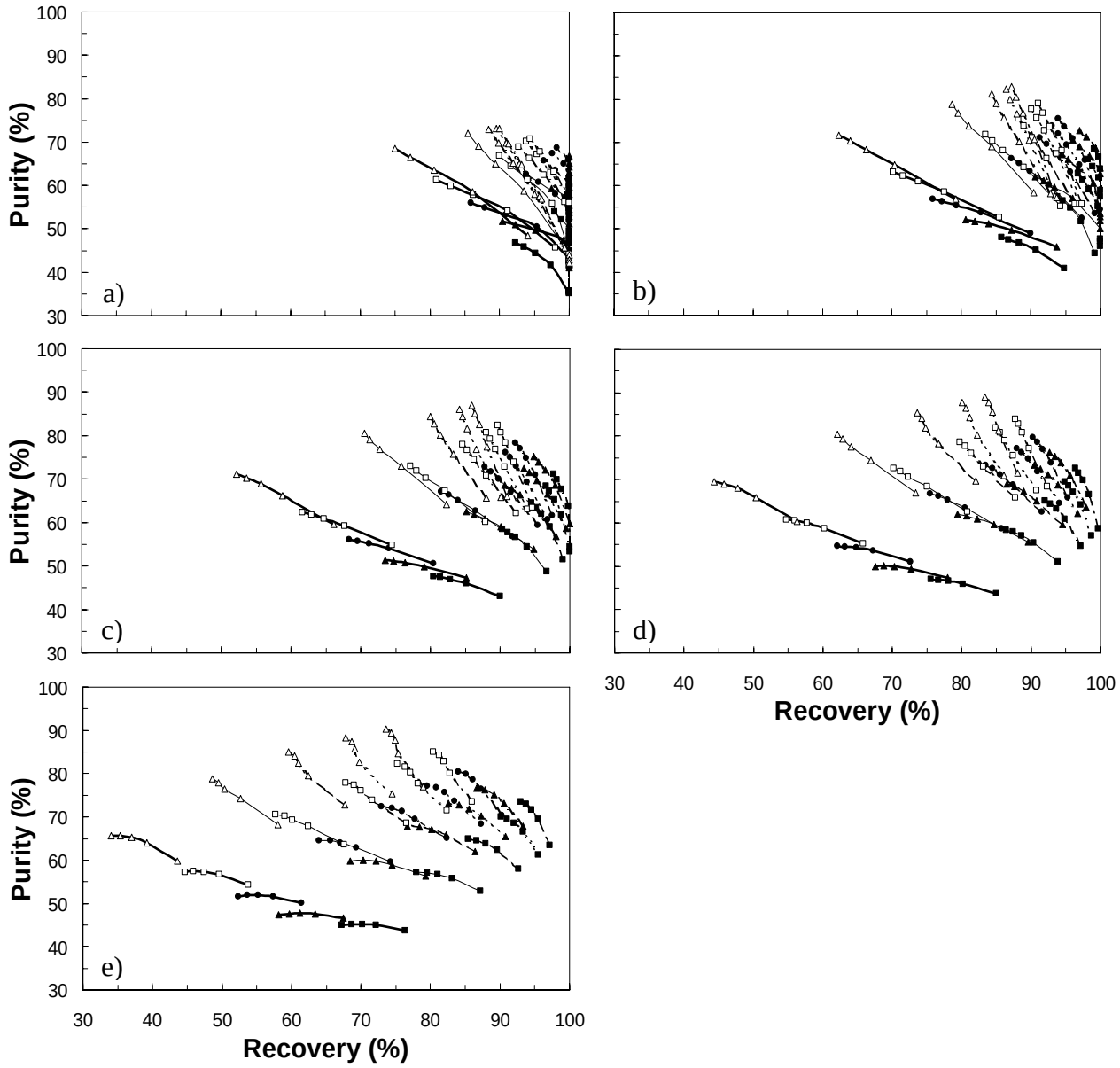

Figure 12. Comparison of performance curves obtained by increasing both the adsorption and desorption mass transfer coefficients by factors of five for the 5-bed stripping PSA cycle with LR and HR from purge for $\gamma = 0.5$ and θ = a) 5.8 L STP/hr/kg, b) 11.2 L STP/hr/kg, c) 17.3 L STP/hr/kg, d) 23.1 L STP/hr/kg and e) 34.6 L STP/hr/kg. Each line corresponds to five runs with t_s increasing from right to left. Lines: bold – $\pi_T = 4$; thin – $\pi_T = 6$; dashed – $\pi_T = 8$; dotted – $\pi_T = 10$; dot-and-dash – $\pi_T = 12$. Symbols: filled squares – RR = 0.0; filled triangles – RR = 0.2; filled circles – RR = 0.4; empty squares – RR = 0.6; empty triangles – RR = 0.8.

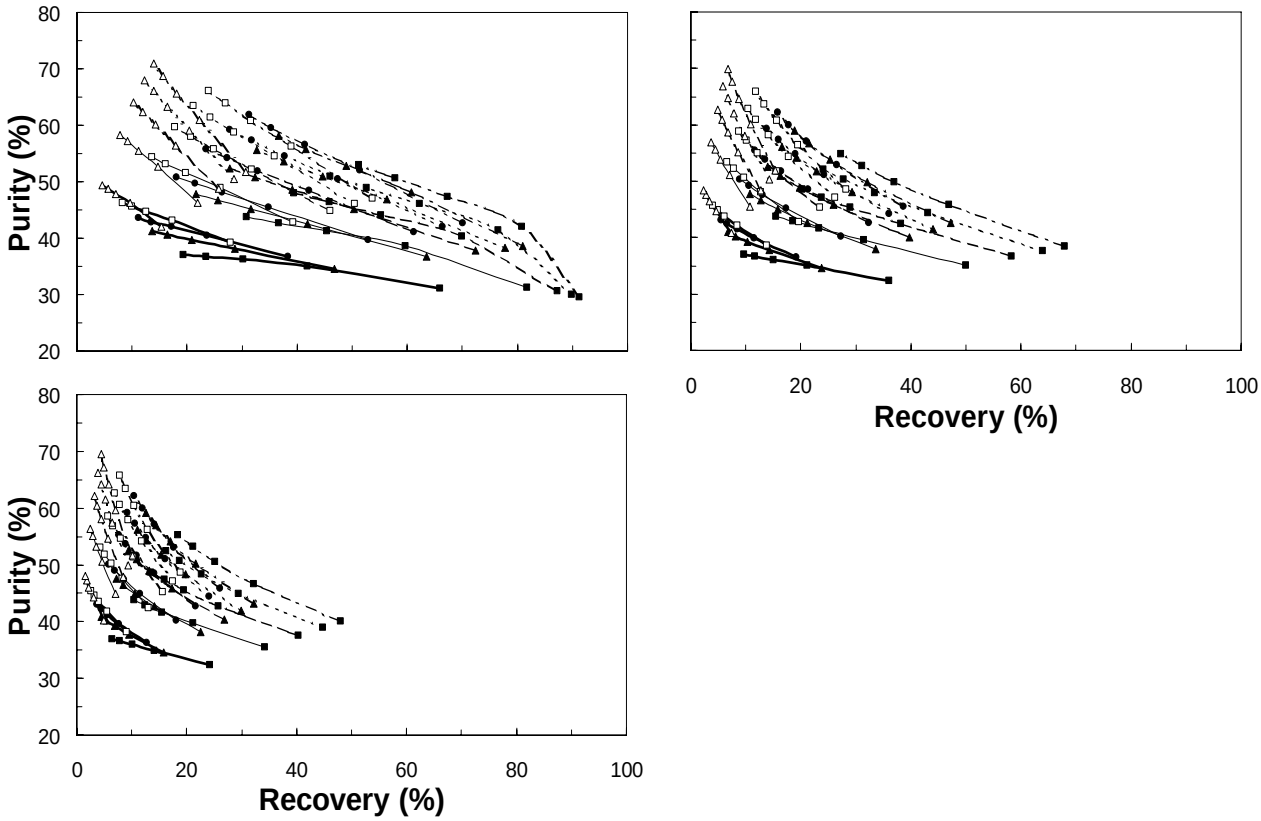

Figure 13. Comparison of performance curves for the 4-bed stripping PSA cycle with HR from depressurization for γ = 0.5 and θ = a) 5.8 L STP/hr/kg, b) 11.2 L STP/hr/kg and c) 17.3 L STP/hr/kg. Each line corresponds to five runs with t_s increasing from right to left. Lines: bold – π_T = 4; thin – π_T = 6; dashed – π_T = 8; dotted – π_T = 10; dot-and-dash – π_T = 12. Symbols: filled squares – RR = 0.0; filled triangles – RR = 0.2; filled circles – RR = 0.4; empty squares – RR = 0.6; empty triangles – RR = 0.8.